

**KAUNAS UNIVERSITY OF TECHNOLOGY
MECHANICAL ENGINEERING AND DESIGN FACULTY**

ARUN GOPINATHAN

**STUDY OF TELESCOPIC INTERMEDIATE STEERING SHAFT
JOINT PERFORMANCE**

Final project for Master degree

Supervisor

Assoc. Prof. Dr Rasa Kandrotaitė
Janutiene

KAUNAS, 2017

KAUNAS UNIVERSITY OF TECHNOLOGY
MECHANICAL ENGINEERING AND DESIGN FACULTY

I APPROVE

Head of Department

(signature) Assoc. Prof. Dr Vytautas Grigas

STUDY OF TELESCOPIC INTERMEDIATE STEERING SHAFT
JOINT PERFORMANCE

Final project for Master degree
MECHANICAL ENGINEERING AND DESIGN (code 621H30001)

Supervisor

(signature) Assoc. Prof. Dr Rasa Kandrotaitė
Janutiene

(date)

Reviewer

(signature) Assoc. Prof. Dr Paulius Griškevičius

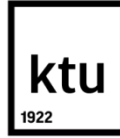
(date)

Project made by

(signature) Arun Gopinathan

(date)

KAUNAS, 2017



KAUNAS UNIVERSITY OF TECHNOLOGY
MECHANICAL ENGINEERING AND DESIGN

(Faculty)

ARUN GOPINATHAN

(Student's name, surname)

Mechanical Engineering and Design, 621H30001

(Title and code of study programme)

**STUDY OF THE TELESCOPIC INTERMEDIATE STEERING SHAFT JOINT
PERFORMANCE**

Final Project

Declaration of academic honesty

_____ January 2017
_____ Kaunas

I confirm that a final project by me, **Arun Gopinathan**, on the subject " study of telescopic intermediate steering shaft joint performance" is written completely by myself; all provided data and research results are correct and obtained honestly. None of the parts of this thesis has been plagiarised from any printed or Internet sources, all direct and indirect quotations from other resources are indicated in literature references. No monetary amounts not provided for by law have been paid to anyone for this thesis.

I understand that in case of a resurfaced fact of dishonesty penalties will be applied to me according to the procedure effective at Kaunas University of Technology.

(name and surname filled in by hand)

(signature)

KAUNAS UNIVERSITY OF TECHNOLOGY
FACULTY OF MECHANICAL ENGINEERING AND DESIGN

Approved:

Head of _____ (Signature, date)

Mechanical
Engineering
Department

Vytautas Grigas

(Name, Surname)

Head of Study _____ (Signature, date)

Programmes in the
Field of Mechanical
Engineering

Kęstutis Pilkauskas

(Name, Surname)

MASTER STUDIES FINAL PROJECT TASK ASSIGNMENT
Study programme MECHANICAL ENGINEERING - 621H30001

Approved by the Dean's Order No. V25-11-7 of January 11th, 2017 y

Assigned to the student **Arun Gopinathan**

(Name, Surname)

1. Title of the Project

STUDY OF TELESCOPIC INTERMEDIATE STEERING SHAFT JOINT PERFORMANCE

2. Aim of the project

The aim of the project is to improve the design of the commercially applicable automotive telescopic splined steering shaft and to analyse the contact stress for reducing wear associated with

3. Tasks of the project

- Select and investigate the telescopic intermediate steering spline shaft which undergoes frequent failure.
- Find the material composition of the selected shaft which faces the failure by chemical analysis.
- Measurement of the major diameter of the external and internal spline shaft is done to calculate the other dimensions of the shaft.
- Theoretical model of the shaft is designed and the dimensions are calculated model the shaft based on both ANSI and ISO the standards [1].
- The dimension of the shaft is measured by doing iteration and modeling from the image which has taken for the inspection. This experimental value is used to model the experimental model.
- Based on the comparison of calculated model and the experimental model, the tolerance class in the standards and fit class used are noted.
- Different models are created based on four variations such as the module, teeth shape, different pressure angles and tolerance and fit class values used at the tooth of the shaft.
- Perform Static Structural analysis to find the improved design which gives better results in all the models under four variations provided
- Compare the results of the improved model obtained with the experimental model and find

4. Specific Requirements

No specific requirements

5. This task assignment is an integral part of the final project

6. Project submission deadline: 2017 January 11th

Task Assignment received

Arun Gopinathan

(Name, Surname of the Student)

(Signature, date)

Supervisor

Assoc. Prof. Dr Rasa Kandrotaitė Janutiene

(Position, Name, Surname)

(Signature, date)

Gopinathan, Arun. Teleskopinio jungiamojo vairo veleno sujungimo parametrų tyrimas. Magistro baigiamasis projektas/vadovas doc. dr. Rasa Kandrotaitė Janutiene; Kauno technologijos universitetas, Mechanikos inžinerijos ir dizaino fakultetas.

Studijų kryptis ir sritis: Mechanikos inžinerija, Technologijos mokslai.

Reikšminiai žodžiai: trintis, jungiamasis vairo velenas, FEM, išdrožos, įtempiai

Kaunas, 2017. 69 p.

SANTRAUKA

Jungiamasis vairo velenas yra naudojamas vairo kolonėlės mechanizme siekiant užtikrinti geresnę vairo reakciją perduodant judesius iš vairo į vairo pavarą. Nors yra daug įvairių jungiamųjų vairo velenų dizaino rūšių, automobilių gamintojų tarpe plačiausiai yra naudojami teleskopiniai išdrožiniai velenai dėl gero sukimosi stiprumo ir atsparumo ašinei apkrovai. Jie sudaryti iš išorinio gaubiamojo vamzdžio ir vidinio veleno, sujungtų išdrožinėmis jungtimis, kurios veikia kaip blokavimo įtaisai.

Šiandien transporto priemonių gamintojai, naudojantys, C-eps tipo vairo kolonėlių mechanizmus, dažnai sulaukia grąžinamų transporto priemonių dėl vairo veleno remonto ir keitimo. Pagrindinis gedimas, atsirandantis eksploatuojant vairo velenus su išdrožinėmis jungtimis, yra deformacijos išdrožose, kai vairas yra dažnai ir staigiai sukamas važiuojant mažu greičiu. Ši deformacija yra trinties ir netinkamos sukimo jėgos, veikiančios išdrožas, rezultatas. Dėl šių priežasčių didėja tarpelis išdrožinėje jungtyje, kuris sukelia triukšmą ir vairo mechanizmo gedimą.

Šio tiriamojo darbo tikslas yra nustatyti sukimosi ir kontaktinių įtempių įtaką vairo veleno stiprumui ir atsparumui trinčiai ir pasiūlyti patobulintą jo dizainą, leidžiantį pagerinti jo mechanines charakteristikas. Darbe pateikiama teleskopinio išdrožinio jungiamojo vairo veleno, naudojamo lengvuosiuose automobiliuose, analizė ir projektavimas baigtinių elementų metodu (FEM). Veleno modelis buvo sukurtas atsižvelgiant į komercinių naudotų transporto priemonių velenų matmenis, pasinaudojant programine įranga SolidWorks. Buvo atlikta naudotų velenų cheminė analizė siekiant nustatyti medžiagos tipą ir galimas savybes. Modeliuojant FEM, buvo

pastebėta, kad didėjant sukimo momentui didėja kontaktiniai išdrožų įtempiai, sukiantys deformacijas ir padidėjusią trintį.

Gopinathan, Arun. Study of telescopic intermediate steering shaft joint performance. Masters in Mechanical Engineering Supervisor final project/supervisor Assoc. Prof. Dr. Rasa Kandrotaitė Janutiene; Kaunas University of Technology, Mechanical Engineering and Design faculty, Mechanical Engineering department.

Study area and field: Mechanical Engineering, Technological Sciences

KEYWORDS: Wear, intermediate steering shaft, FEM, spline teeth, stress

Kaunas, 2017, 69 p.

SUMMARY

The intermediate steering shaft used in the steering system is used widely based on providing better steering response by transmitting the motion from steering wheel to the steering gear. The steering wheel inside the driver compartment is connected with the one end of the shaft and the other end of the shaft is connected to the gear. Though various types of intermediate shaft available, telescopic splined shaft are widely preferred by the manufacturers for good torsional strength and axial loading condition. It has an outer and inner splined shaft in which the spline in this shaft acts as a tubular locking device. These splines connect the extension shaft to the steering gearbox.

Nowadays the vehicle manufacturers using C-Eps steering are doing frequent recalling of the vehicle for repair and replacement of the steering shaft. The major defect that could happen with the splined shaft is the occurrence of deformation of the splines if the steering wheel is frequently and forcefully rotated while driving at low speed. This deformation is the result of excessive wear and inadequate torsional strength in the splines. It ultimately leads to the increase in backlash or clearance which causes the noise and faulty steering. In case of accidents, increased loading will cause bending of the shaft due to the lack of strength.

The scope of this research paper is on finding the influence of applied torque on the contact stress developed and its impact on the wear resistance of the splined shaft. It deals with the design and analyses the telescopic splined intermediate steering shaft used in automotive by the finite element analysis method. The design has been made with measured dimensions of a commercially used vehicle intermediate shaft through SolidWorks. Chemical analysis was done to find the material and its properties that have used in the shaft commercially. From the

analysis made through FEA method, it has been observed that the increase in torque has a greater influence on the increase in contact stress-strain properties which leads to wear.

ACKNOWLEDGEMENT

I take it as a privilege to express my profuse thanks to my beloved advisor Assoc. Prof. Dr. Evaldas Narvydas of Mechanical Engineering and Design department, for his kind guidelines and support which allow me for completing the final semester project.

We extend our hearty thanks to Lithuanian Energy Institute who had help me on finding the chemical analysis necessary for the project.

I am thankful to the project supervisor, Assoc. Prof. Dr Rasa Kandrotaitė Janutiene of Mechanical Engineering and Design department, who encourages me to complete the project successfully.

TABLE OF CONTENTS

| | |
|--|----|
| INTRODUCTION | 6 |
| PROBLEM DEFINITION | 7 |
| AIM..... | 8 |
| TASK TO BE PERFORMED..... | 8 |
| 1. LITERATURE REVIEW | 9 |
| 1.1 Importance of Torque..... | 9 |
| 1.2 Involute Splines..... | 10 |
| 1.2.1 Spline Shape | 12 |
| 1.2.2 Involute Spline- Error Patterning | 12 |
| 1.2.3 Types of Error..... | 13 |
| 1.3 Spline Fit and Clearance | 13 |
| 1.3.1 Major Diameter Fit | 13 |
| 1.3.2 Minor Diameter Fit..... | 14 |
| 1.3.3 Side Fit..... | 15 |
| 1.3.4 Tolerance Class and its importance | 17 |
| 1.4 Shear Stress on Involute Spline Profile..... | 17 |
| 1.5 Involute splines and Gear | 21 |
| 1.6 Spline Tooth Structure Design and Advantages | 22 |
| 1.6.1 Spline Teeth Engagement..... | 23 |
| 1.7 Manufacturing | 24 |
| 1.8 Tooth Deviation..... | 24 |
| 1.9 Spline Teeth and Applications | 27 |
| 1.10 Wear in the spline shaft..... | 27 |

| | |
|---|----|
| 1.11 Importance of Hardness in the Splined Shaft..... | 28 |
| 2. CHEMICAL ANALYSIS..... | 30 |
| 2.1 Material in Use..... | 30 |
| 2.1.1 Brucker Q4Tasman..... | 30 |
| 2.1.2 Spectroscopic Analysis..... | 30 |
| 2.1.3 Sample for Chemical Analysis..... | 31 |
| 2.2 Steps Involved in Analysis..... | 31 |
| 2.3 Metallurgical Characterization..... | 32 |
| 2.3.1 Materials..... | 32 |
| 3. DESIGN METHODOLOGY..... | 34 |
| 3.1 Pressure Angle Inspection..... | 35 |
| 3.2 Influence of design and analysis:..... | 36 |
| 3.3 Experimental Shaft..... | 36 |
| 3.4 Calculation Based on the Standards..... | 37 |
| 3.5 Mathematical Design Calculations..... | 40 |
| 3.5.1 Internal Spline shaft..... | 40 |
| 3.5.2 External Spline shaft..... | 41 |
| 4. DESIGN IMPROVEMENT..... | 44 |
| 4.1 Improvement based on Module..... | 44 |
| 4.2 Improvement based on the Fit Tolerance..... | 44 |
| 4.3 Improvement based on the Tooth Shape..... | 46 |
| 4.4 Improvement based on the Pressure Angle..... | 46 |
| 5.FINITE ELEMENT STUDY AND ANALYSIS..... | 48 |
| 6.RESULTS..... | 50 |
| 6.1 Based on the Module..... | 50 |

| | |
|--|----|
| 6.2 Based on the Pressure Angle..... | 52 |
| 6.3 Based on the Tolerance | 54 |
| 6.4 Based on the shape | 56 |
| 6.5 Improved Model..... | 58 |
| 6.6 Comparison of Mises Stress of the Experimental and Improved Model under load | 60 |
| 6.7 Comparison of Equivalent Strain of the Experimental and Improved Model under load... | 61 |
| 6.8 Comparison of Total Deformation of the Experimental and Improved Model under load. | 62 |
| 7.CONCLUSION..... | 63 |
| 8.FUTURE SCOPE..... | 65 |
| REFERENCE..... | 66 |
| APPENDIXES | 68 |

LIST OF FIGURES

| | |
|---|----|
| Figure 1: Telescopic splined intermediate steering shaft..... | 7 |
| Figure 2: Schematic View of the Steering system and Torque generation..... | 9 |
| Figure 3: Torque Generated on various steering system [19]..... | 10 |
| Figure 4 : A rigid bar rolling on a fixed cylinder [9]..... | 11 |
| Figure 5: Generating an involute curve from a base circle [14] | 11 |
| Figure 6: Types of Error [10]..... | 13 |
| Figure 7: Major Diameter Fit [11] | 14 |
| Figure 8 : Minor Diameter Fit [11]..... | 14 |
| Figure 9: Side Fit [11]..... | 15 |
| Figure 10:Spline Tooth side mating members [11] | 21 |
| Figure 11:Gear tooth Mating (a) vs Involute spline shaft Mating (b) [21]..... | 22 |
| Figure 12: Spline Terms, Symbols, and Drawing Data, 30-Degree Pressure Angle, Flat Root Side Fit ANSI B92.1-1970, R1993 [1] | 23 |

| | |
|--|----|
| Figure 13:Actual and effective tooth thickness [2]..... | 25 |
| Figure 14:Tolerance zones for the tooth thickness and the space width..... | 26 |
| Figure 15:Wear Pattern [18] | 28 |
| Figure 16:Spline tooth profile of the axial shaft [13] | 29 |
| Figure 17: Brucker Q4Tasman Apparatus Set up..... | 30 |
| Figure 18:Sample Prepared for Chemical Analysis..... | 31 |
| Figure 19:Cross sectional view of the Spline Shaft..... | 34 |
| Figure 20:Microscopic view of mating member of the telescopic spline shaft. | 35 |
| Figure 21: Comparison of Serration Spline (a) and Involute spline (b) | 46 |
| Figure 22: Geometry of the joint (a); its realization in ANSYS Workbench with the loads and displacement boundary conditions (b) and the view of the finite element mesh (c). | 49 |
| Figure 23:Von-Mises stress developed on the shaft of different modules..... | 51 |
| Figure 24:Maximum Equivalent Strain developed on the shaft of different Modules | 51 |
| Figure 25:Total Deformation on the shaft of different Modules | 52 |
| Figure 26: Von-Mises stress developed on the shaft of different pressure angles..... | 53 |
| Figure 27:Maximum Equivalent Strain developed on the shaft of different pressure angles..... | 53 |
| Figure 28:Total Deformation on the shaft of different pressure angles..... | 54 |
| Figure 29: Von-Mises stress developed on the shaft of different Tolerance variations | 55 |
| Figure 30:Equivalent Strain developed on the shaft of different pressure angles | 55 |
| Figure 31:Total deformation on the shaft of different pressure angles..... | 56 |
| Figure 32:Von-Mises stress developed on the shaft of two different shapes | 57 |
| Figure 33:Maximum Equivalent Stress developed on the shaft of two different pressure angles | 57 |
| Figure 34:Total Deformation on the shaft of two different pressure angles..... | 58 |
| Figure 35: von-Mises Stress developed in the experimental model under load | 60 |
| Figure 36: von-Mises Stress developed in the Improved model under load..... | 60 |
| Figure 37:Equivalent Strain developed in the Experimental model under load | 61 |
| Figure 38:Equivalent Strain developed in the Improved model under load | 61 |
| Figure 39:Total Deformation occurring in the Experimental model under load | 62 |
| Figure 40:Total Deformation occurring in the Improved model under load | 62 |
| Figure 41:Proposed idea with the implementation of splined pad with compression spring | 65 |
| Figure 42: Internal Spline Shaft (a) and External Spline Shaft (b)..... | 68 |

| | |
|---|----|
| Figure 43: Experimental Telescopic Intermediate Splined Shaft | 68 |
| Figure 44: Experimental Model CS | 69 |
| Figure 45: Theoretical Model CS | 69 |
| Figure 46: Model with 0.3 module CS..... | 69 |
| Figure 47: Model with Serration CS..... | 69 |
| Figure 48: Minimum Tolerance Model CS..... | 69 |
| Figure 49: Model with 30 deg CS..... | 69 |

LIST OF TABLES

| | |
|---|----|
| Table 1 : Fit class [12] | 16 |
| Table 2: Form deviation [2] | 27 |
| Table 3: Sample T-Fe..... | 32 |
| Table 4: Material Properties..... | 33 |
| Table 5: Dimension of the experimental Spline Shaft..... | 36 |
| Table 6: Splined Shaft Dimensions..... | 42 |
| Table 7: Dimensions based on the Module..... | 44 |
| Table 8: Dimensions based on the tolerance variations..... | 45 |
| Table 9: Dimensions based on the Pressure Angle..... | 47 |
| Table 10: Stress -Strain results based on the change in module | 50 |
| Table 11: Stress-Strain results based on the change in pressure angle | 52 |
| Table 12: Stress-Strain analysis results based on the change in tolerance | 54 |
| Table 13: Stress-Strain analysis results based on the shape of the teeth | 56 |
| Table 14: Stress-Strain results of the models with improvement | 59 |

INTRODUCTION

Splined connection shafts used for transmitting torque from one rotating member to another are preferably used in rotating machinery as a coupling mechanism. The splined connection used in the automotive intermediate steering shaft has got its importance in the steering system to get a better steering ability, steering response on considering safety reasons and to enhance the comfort of drivers. Every automobile steering system consists of the steering wheel which is connected to the steering shaft assembly and then to the steering device. The steering system starts from the steering wheel located inside the driver compartment of the vehicle which is rotatably supported by the driver. The one end of the steering shaft assembly is connected to the rotating steering wheel and the other end is connected to the steering device for turning the front, and sometimes the rear wheels in response to the rotation of steering wheel. The shaft is supported by a pair of yokes mounted on the end which is connected to the steering wheel and steering device by the proper universal joints.

The intermediate steering shaft is available in various types and different shapes which come under two categories – suitable for impact absorption mechanism and, suitable for vibration and noise absorption mechanism [1]. The splined shaft used in this study belongs to the telescopic spline type intermediate steering shaft. Telescopic spline type intermediate shafts have a greater application in the recent years because of their ease of installation and stability on steering. This type of shaft is equipped with vibration and noise absorption mechanism.

Nowadays, most of the automobile manufacturers are frequently recalling their vehicle for repairing and remounting the intermediate steering shaft due to the uncomfortable steering experience faced by the customers. It is mainly due to the increase in backlash happened in the splines of the telescopic intermediate shaft. So, it is important to focus more on improving the steering experience by avoiding noise and the loss of steering ability happened in the telescopic spline steering shaft which ultimately leads to accidents.

PROBLEM DEFINITION

A telescopic splined type intermediate shaft has an inner splined shaft and a tubular outer shaft fitted in an axial direction. The outer splines are provided on an outer periphery of the inner shaft and the inner splines are provided on an inner periphery of the outer shaft. Spline in this shaft is a tubular locking device which connects the extension shaft to the steering gearbox. The major defect that could happen with the splined shaft is the occurrence of deformation of the splines if the steering wheel is frequently and forcefully rotated while driving at low speed. This deformation is the result of inadequate hardness, excessive wear and corrosion. It ultimately leads to the increase in backlash or clearance which causes the noise and faulty steering. This increase of backlash is also the result of rapid wear of the resin coating [3]. Sliding off the shaft over a long period of time leads to the wear of resin coating which also increases the surface roughness of the shaft in the axial direction.



Figure 1: Telescopic splined intermediate steering shaft

AIM

The aim of the project is to improve the design of the commercially applicable automotive telescopic splined steering shaft and to analyse the contact stress for reducing wear associated with backlash.

TASK TO BE PERFORMED

The major task which is conducted on designing the shaft is given below.

- Select and investigate the telescopic intermediate steering spline shaft which undergoes frequent failure.
- Find the material composition of the selected shaft which faces the failure by chemical analysis.
- Measurement of the major diameter of the external and internal spline shaft is done to calculate the other dimensions of the shaft.
- Theoretical model of the shaft is designed and the dimensions are calculated model the shaft based on both ANSI and ISO the standards [1].
- The dimension of the shaft is measured by doing iteration and modelling from the image which has taken for the inspection. This experimental value is used to model the experimental model.
- Based on the comparison of calculated model and the experimental model, the tolerance class in the standards and fit class used are noted.
- Different models are created based on four variations such as the module, teeth shape, different pressure angles and tolerance and fit class values used at the tooth of the shaft.
- Perform Static Structural analysis to find the improved design which gives better results in all the models under four variations provided
- Compare the results of the improved model obtained with the experimental model and find the model with better performance.

1. LITERATURE REVIEW

Based on the research made by H.Ueda of Koyo Engineering, the increase of column type electric power steering (C-EPS) application in automobiles requires for improved performance of intermediate shafts which transmits the steering response to the steering wheel and then to the wheel. High torque transmission is the major necessity of the shaft in C-EPS system.

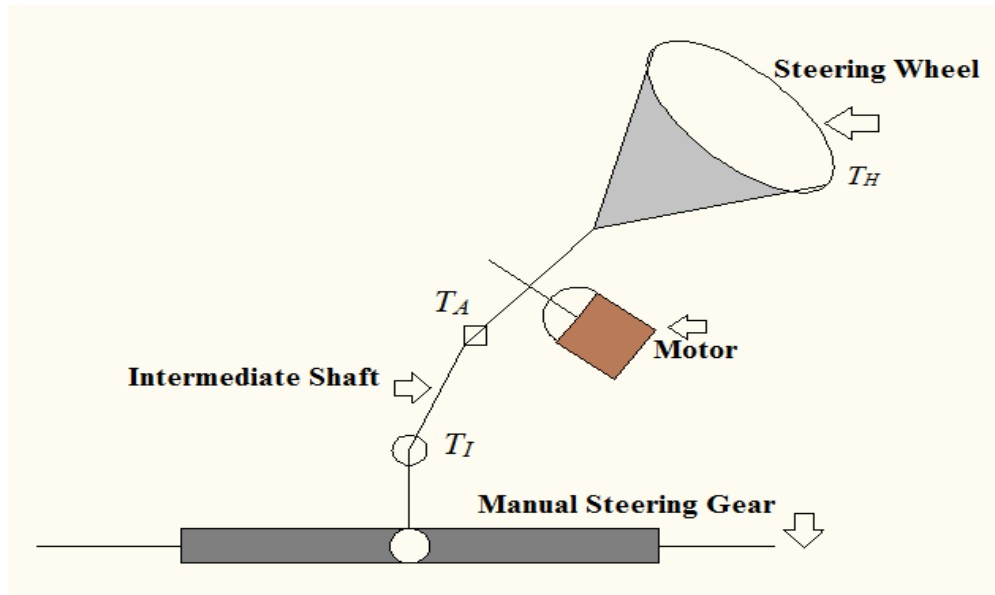


Figure 2: Schematic View of the Steering system and Torque generation

The torque which is transmitted to the steering gear is represented by T_I and it is given by the following equation.

$$T_I = T_H + T_A \quad (1.1)$$

Where T_H is the torque generated due to steering response and T_A is the motor output torque which is generated and multiplied with a ratio of reduction and reduction efficiency of the gear.

1.1 Importance of Torque

In the case of power steering equipped hydraulic system, the force applied on the steering gear is due to the torque on the intermediate shaft. So the value of T_I is same as that of T_H . Based on the application, the maximum torque generated on the intermediate shaft is about 10 Nm [19].

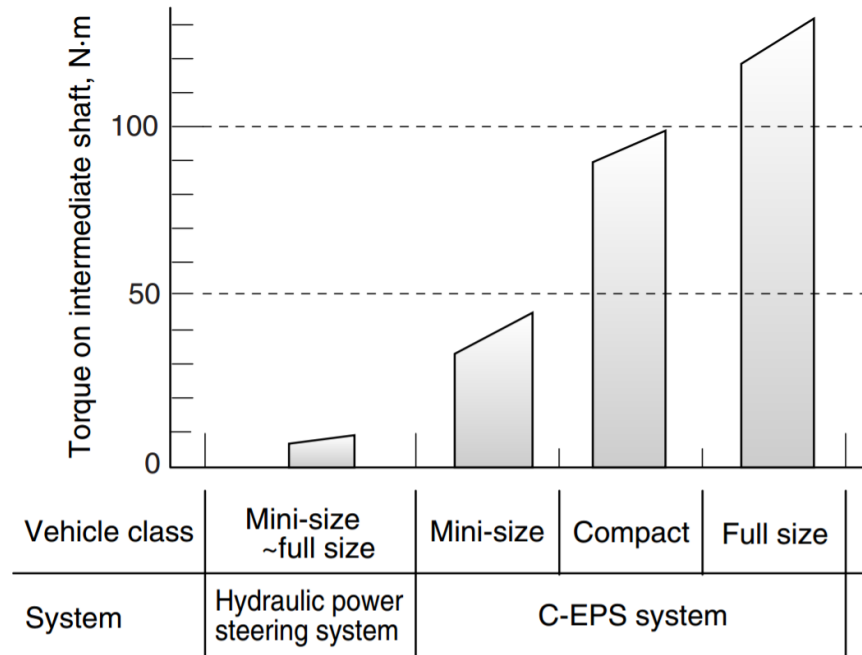


Figure 3: Torque Generated on various steering system [19]

From the figure 1.1.a, it is evident that the C-EPS system experiences more torque on the intermediate shaft comparatively to the hydraulic power steering system. So it is very important to use the intermediate shaft with high torsional rigidity, low sliding load and better durability.

1.2 Involute Splines

The involute profile has the spline teeth which resembles same as that of the gears. Involute is the term that describes the curve of the circle which is described by the end of the line not connected from the circumference of the circle [8]. It has also been defined, when a rigid bar AD creates a path on the fixed base circle without slipping, the path followed by the point A is termed as involute [9].

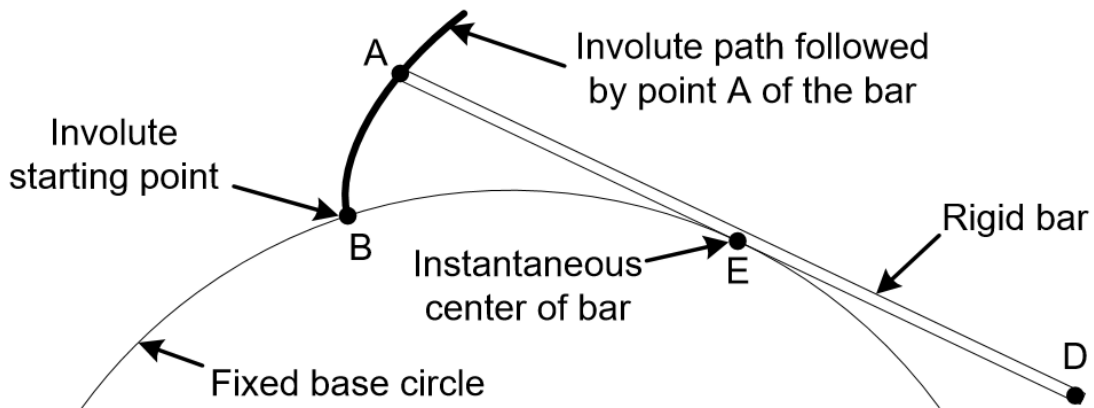


Figure 4: A rigid bar rolling on a fixed cylinder [9]

The basic geometry used to define the involute curve is shown in the figure 1.2.a [10]. Taut-line ρ is used to generate the involute curve which is unwound from the base circle with the radius R_b . The distance between the taut end point p and the base circle center C is given by the radius vector r .

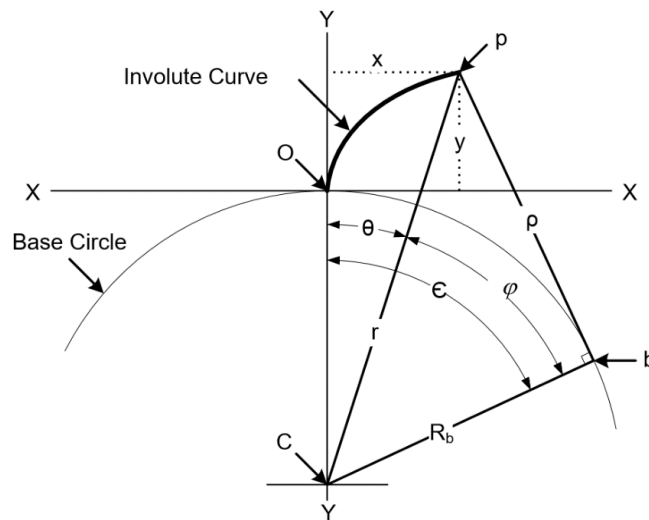


Figure 5: Generating an involute curve from a base circle [14]

The summation of the pressure angle φ and the profile angle θ is called roll angle ϵ . Roll angle is used to determine the coordinates of the point p. Some of the useful equations used to determine the coordinates of the point on the involute curve are given below.

$$\rho = R_b(\theta + \varphi) \quad (1.2)$$

$$x = R_b \sec \varphi \sin \theta \quad (1.3)$$

$$y = R_b(\sec \varphi \cos \theta - 1) \quad (1.4)$$

An involute curve is an important form of spline profile which provides more benefit than the straight-sided splines. It is more convenient to cut and fit with tolerance.

1.2.1 Spline Shape

Widely applicable splined shaft has the splines of straight and involute shape. Straight splined shafts are commonly used in many applications however, the splined shaft with involute splines has a steady increase in its application because of its greater torque transmitting capacity and self-centering action. As backlash between the fixed mating members of the telescopic splined intermediate steering shaft is the major reason for the steering failure, the involute splines which give better self-centering action under loads is preferred. It was found that the shaft in this research which faces the frequent failure also have involute splines.

Involute serration is a term often applicable to the splines with the standard pressure angle of 30° , 37.5° and 45° [1]. For some special applications especially in gear tooth, 14.5° , 20° and 25° pressure angles are used [2].

1.2.2 Involute Spline- Error Patterning

The review related with the geometry of the involute, hob and necessary hobbing process, and application of splines which involve complex geometry of splines, processing technology and mathematics has been made to understand the error patterning happened in the splines. Error patterning is used in special applications like brakes used in industries which help to increase the tooth engagement. It allows multiple teeth engagement at a time which distributes the total load acting on a tooth and increases the load carrying capacity. Thus, error patterning helps the designers to design the spline teeth with better load applications.

1.2.3 Types of Error

The errors related with the spline geometry are categorised into four different categories – Profile error, tooth thickness error, Index error and Radial error [10].

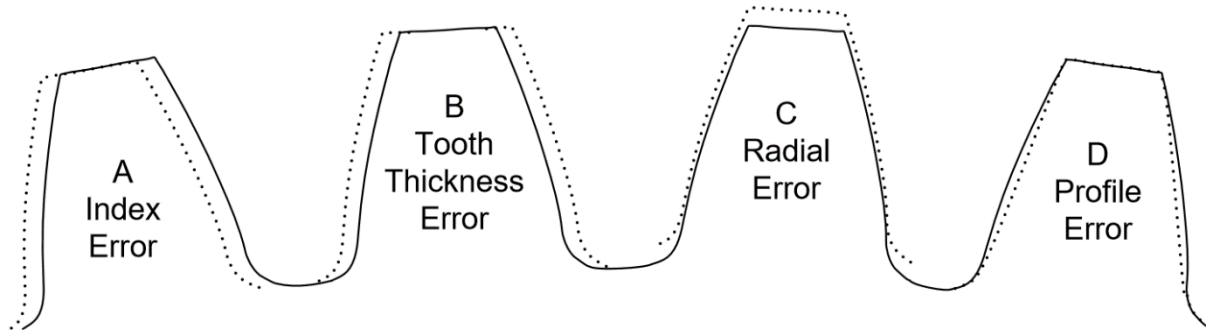


Figure 6: Types of Error [10]

It is important to know the error and its sources to understand the variation of the tooth clearance and sequence of engagement on the application. Finding the tooth errors is a difficult task due to the geometry of the tooth and the error happening is very small. Sensitive equipment and great care must be needed on experimental setup to get the high resolution on detecting the tooth errors and spline engagement.

1.3 Spline Fit and Clearance

Based on the Indian standard developed by Bureau of standards [11], there are three types of fit which can be used for involute spline types. They are major diameter fit, minor diameter fit and side fit.

1.3.1 Major Diameter Fit

From the name itself, this kind of fit has equal diameter value for the major diameter for both internal and external splines. The tooth clearance will be provided as a circular clearance between the space width of the internal spline and the tooth thickness of the external spline.

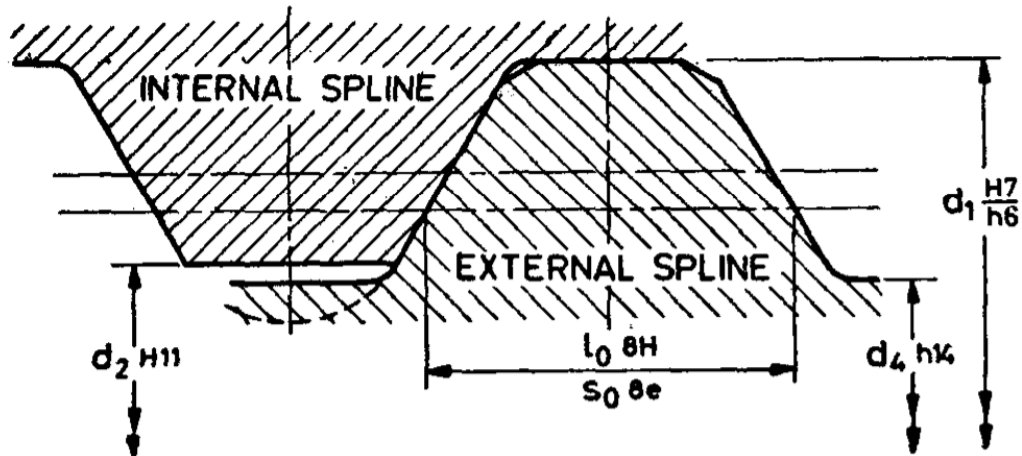


Figure 7: Major Diameter Fit [11]

From the figure 1.3.a, the tolerance value for the internal spline recommended from the standard H11 which is provided to the minor diameter and the tolerance value provided for the external spline is h14.

1.3.2 Minor Diameter Fit

In this kind of fit, the minor diameter for both internal and external splines is same. The circular clearance is provided between the space width of the internal spline and the tooth thickness of the external spline.

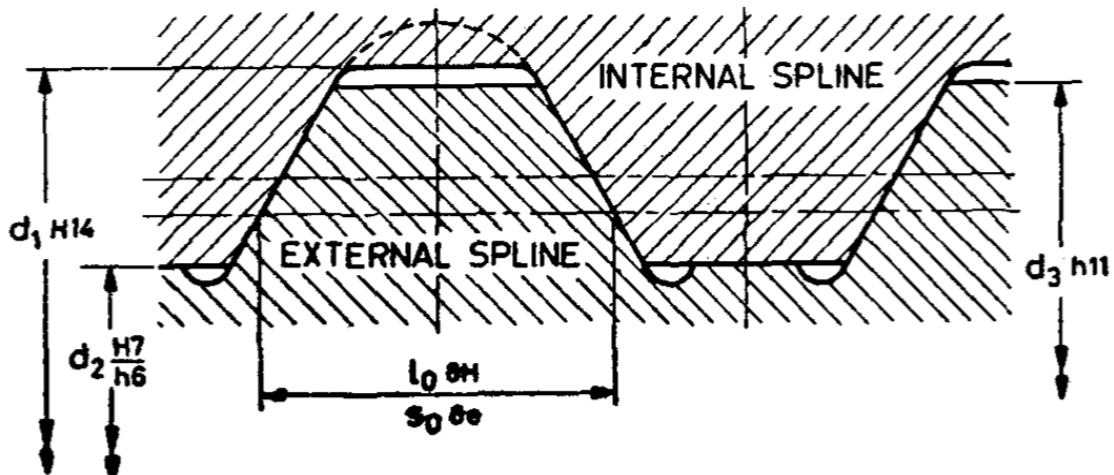


Figure 8: Minor Diameter Fit [11]

From the figure 1.3.b, the tolerance value for the internal spline recommended from the standard H14 which is provided to the major diameter and the tolerance value provided for the external spline is h11.

1.3.3 Side Fit

Side fit is a special kind of fit in which the teeth of the internal and the external splines have contacts on the sides of the teeth only. In this kind of fit, the tolerance value is provided to both the major and minor diameter of the internal and external splines.

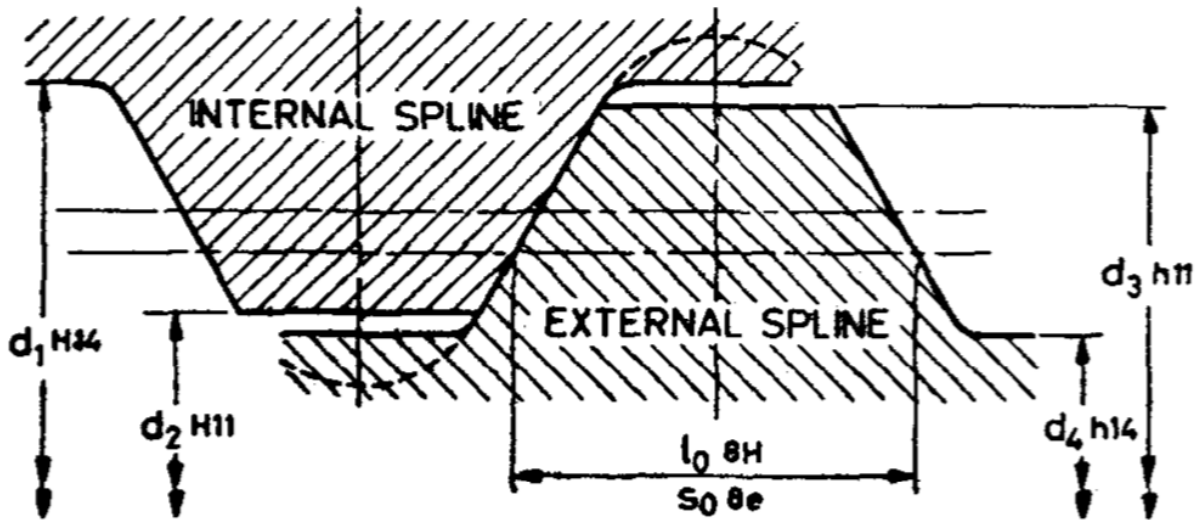


Figure 9: Side Fit [11]

From the figure 1.3.c, the tolerance class H14/h11 is provided to the internal splines and H11/h14 is provided to the external splines. Based on the tolerance, the fit is also classified as press fit, locating fit and sliding fit.

Table 1: Fit class [12]

| | Hole Basis | Shaft Basis | Description |
|------------------|------------|-------------|--|
| Clearance Fit | H11/c11 | C11/h11 | Loose running fit for wide commercial tolerances or allowances on external members. |
| | H9/d9 | D9/h9 | Free running fit not for use where accuracy is essential but good for large temperature variations, high running speeds, or heavy journal pressures. |
| | H8/f7 | F8/h7 | Close running fit for running on accurate machines and for accurate location at moderate speeds and journal pressures. |
| | H7/g6 | G7/h6 | The sliding fit not intended to run freely, but to move and turn freely and locate accurately. |
| Transition Fit | H7/h6 | H7/h6 | Locational clearance fit provides a snug fit for locating stationary parts but can be freely assembled and disassembled. |
| | H7/k6 | K7/h6 | Locational transition fit for accurate location, a compromise between clearance and interference. |
| Interference Fit | H7/n6 | N7/h6 | Locational transition fit for the more accurate location where greater interference is permissible. |
| | H7/p6 | P7/h6 | The locational interference fit for parts requiring rigidity and alignment with a prime accuracy of location but without special bore pressure requirements. |
| | H7/s6 | S7/h6 | Medium drive fit for ordinary steel parts or shrink fits on light sections, the tightest fit usable with cast iron. |
| | H7/u6 | U7/h6 | Force fit suitable for parts which can be highly stressed or for shrink fits where the heavy pressing forces required are impractical. |

*Transition fit for basic sizes in range from 0 through 3 mm

1.3.4 Tolerance Class and its importance

Mostly the tolerance is selected and is applied to the space width and tooth thickness of the spline teeth. Based on the Standards ASA B 5.15 – 1960 [1], the machining tolerance value for the spline fit is classified into four classes and it was categorised by the numbers 4,5,6 and 7. The tolerance class is calculated by the following formulas.

$$\text{Class 4} = 0.71 \times \text{Class 5} \quad (1.5)$$

$$\text{Class 6} = 1.40 \times \text{Class 5} \quad (1.6)$$

$$\text{Class 7} = 2.00 \times \text{Class 5} \quad (1.7)$$

The dimensions which one can get are the dimensions after the part is manufactured. So, the compensation made on doing processing such as machining and heat treatment are considered before the tolerance value for manufacturing is selected.

On selecting the tolerance value from the standards, the minimum effective space width of the internal splines and the maximum effective tooth thickness of the external splines are same and two types of fit are considered. In some cases, the tolerance class “mix” of the mating members is considered [1]. It has the average tolerance value of two classes and it is easy to manufacture. The standard provided for the involute spline is not applicable in the case of press fit conditions. In the case of a press fit, the space width of the internal spline is kept constant and the changes have been provided to the external spline tooth thickness and the diameter.

Based on the ISO system of limits and fits [12] and the tolerance analysis [2], various fit classes such as H/d, H/e, H/f, H/h, H/js and H/k are considered. This fit classes mentioned is only to consider the side fits. The coaxial connection is created simultaneously when the torque is transmitted by the tooth flanks.

1.4 Shear Stress on Involute Spline Profile

The results of the stress obtained in this research are related to the stress at the mating surface which leads to the wear problem. The three-dimensional models are dealt in some article to analyse the splines with the global boundary conditions. Two-dimensional modelling is used to study most of the spline models.

Based on the standards, the analytical model was predicted to find the torque and stresses developed on the spline connections. Basically, the axial stress in the circular cross section of the rigid solid bar due to bending is calculated by the following formula:

$$\sigma = \frac{My}{I} \quad (1.8)$$

Where σ is the axial stress developed normal to the plane of cross section of the bar, y is the distance, M is the applied moment to the bar. I is the moment of inertia for the circular cross section and it is given by:

$$I = \frac{\pi r^4}{4} \quad (1.9)$$

The stress mainly shear stress developed in a bar due to the torsional load applied to the circular cross section is provided by the following formula:

$$\tau = \frac{Tr}{J} \quad (1.10)$$

Where τ represents the shear stress due to torsional load, r is the radial distance, T is the torque applied to the bar and J is the polar moment of inertia which was given by the following formula:

$$J = \frac{\pi r^4}{2} \quad (1.11)$$

Based on the bending and torsion ratio, the Von-Mises stress is calculated by the combination of above equations. Von Mises Stress is used to represents the overall magnitude of stress at a given point, regardless of the orientation. It is an equivalent, or effective stress and it is given by the following equation [5]:

$$\sigma' = \frac{1}{\sqrt{2}} [(\sigma_x - \sigma_y)^2 + (\sigma_y - \sigma_z)^2 + (\sigma_z - \sigma_x)^2 + 6(\tau_{xy}^2 + \tau_{yz}^2 + \tau_{zx}^2)]^{1/2} \quad (1.12)$$

The above equation explains the stress at a point in the shaft in the three-dimensional state. In the model, the stress at the contact point due to interference and the shear stress due to torsion is considered. The assumption made is that the material exhibits the mechanical behaviour is homogeneous and isotropic. Also, the shear stress which varies only radially from the axis of the

splined shaft is considered and the stress due to transverse load is neglected. So, the Von Mises stress equation is reduced to:

$$\sigma' = \sqrt{\sigma_z^2 + 3\tau_{zx}^2} \quad (1.13)$$

Where σ' is the magnitude of the von Mises stress, σ_z is the axial stress built due to bending and τ_{zx} is the shear stress developed due to the applied torque.

To calculate the von Mises stress, Algor also provides the similar equation [6]:

$$\sigma_e = \sqrt{0.5[(\sigma_x - \sigma_y)^2 + (\sigma_y - \sigma_z)^2 + (\sigma_z - \sigma_x)^2] + 3(\tau_{xy}^2 + \tau_{yz}^2 + \tau_{zx}^2)} \quad (1.14)$$

Based on the book of Cedoz and Chaplin, "The Design Guide to Involute Splines" [7], they narrate the common details about the design procedures of spline joint connections. From their work, they have provided the formula to calculate the shear stress at the root of the teeth of splines which was more close to the standard for splines ANSI B92.1 1970, R1993.

$$S_s = \frac{2T}{DN_e L_g t} \quad (1.15)$$

Where S_s represents the shear stress developed at the root of the tooth, D gives the diameter of the pitch, T is the applied torque at the spline shaft, N_e is the actual number of teeth in contact, t is the thickness of the tooth at the pitch diameter, and L_g represents the tooth engagement length. Since the equation provided related more on providing the shear stress at the actual engagement of the teeth of the external and internal splines, the equation provided is more relevant to the present study in this research work. When the spline tooth is subjected to pure torsion condition, the nominal shear stress developed at the root is provided by the following equation.

$$S_t = \frac{32TD_{re}}{\pi(D_{re}^4 - D_{in}^4)} \quad (1.16)$$

Where S_t is the shear stress under torsion, D_{re} is the minor diameter of the external splined shaft and D_{in} is the minor diameter of the internal splined shaft. Since the above equation 1.16 is applicable to the external splines with the teeth on the inner diameter of the shaft, it is useful for this present research work.

From the Machinery Handbook of involute splines and serrations [1], the value of torsional shear stress developed under the root diameter of the external splines in the solid spline shaft is given by the following equation:

$$S_s = \frac{16TK_a}{\pi D_{re}^3 K_f} \quad (1.17)$$

Where T is the transmitted torque, K_a is the application factor which was provided from the standard value, K_f is the fatigue life factor taken from the standard value. On keeping K_a and K_f value to unity, the above equation 1.17 is reduced to:

$$S_s = \frac{16T}{\pi D_{re}^3} \quad (1.18)$$

The above equation is dedicated only for the solid shaft and not used for the hollow shaft.

Shear stress developed at the pitch diameter of the teeth for the torque transmitted is calculated based on the literature [1] and it is given by,

$$S_s = \frac{4TK_a K_m}{DNL_e t K_f} \quad (1.19)$$

Where K_m is the load distribution factor, D is the pitch diameter, L_e is the maximum effective length, N is the number of teeth and t is actual tooth thickness. The factor 4 in the equation denotes that the load has been carried by half the teeth because of spacing errors. In the case of poor manufacturing accuracies, the factor of 6 is used instead of 4.

Comparatively to the gear teeth, the compressive shear stress is very lower since non-uniform load distribution and misalignment result in unequal load sharing and end loading of the teeth [1]. In this research, the spline used is in the fixed state and the compressive stress provided is:

$$S_c = \frac{2TK_m K_a}{9DNL_e h K_f} \quad (1.20)$$

Where h is the depth of engagement of the teeth [1] and it was approximately 1/P for fillet root splines.

1.5 Involute splines and Gear

Splines structure designed as an equally spaced tooth connector with variation in the number of teeth. These connector elements are more commonly in use in mechanical elements such as automobile transmission shaft, turbine shaft, gears, pulley, flywheel etc., Based on the working condition, splines are classified as fixed splines and flexible splines[2]. Flexible splines allow the relative motion between the coupling elements and there is no relative motion between the non-flexible or fixed spline. In the case of shaft and hub arrangement, the self-centring action is provided by the involute splines under different load conditions.

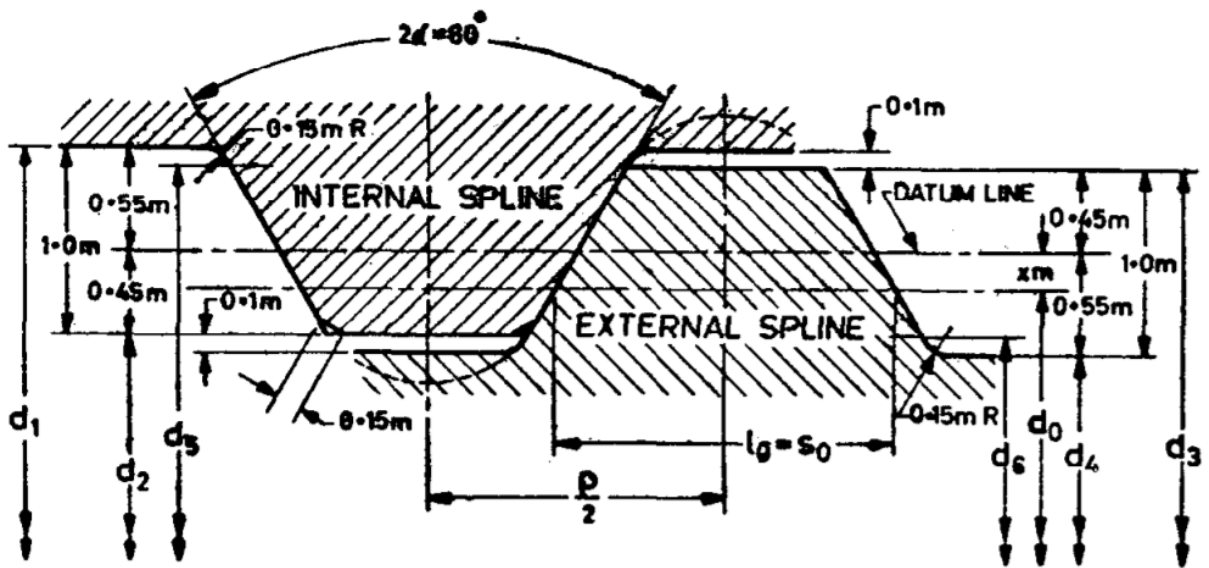


Figure 10: Spline Tooth side mating members [11]

Spline teeth are designed as shorter with pressure angles greater than the gears. These shorter teeth are designed to carry higher loads. The spline teeth are used mostly for coupling action to keep the internal and external spline shaft fixed relative to each other. All the teeth in the splines are engaged to transmit the torque which is different from the torque transmission happening in gear. The internal and external spline shaft assists the coupling to transfer the torque without slipping.

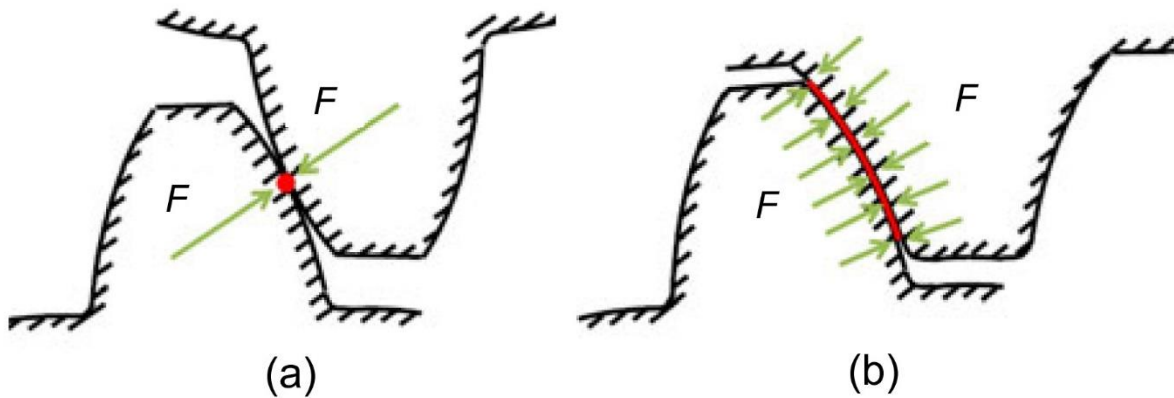


Figure 11: Gear tooth Mating (a) vs Involute spline shaft Mating (b) [21]

Gears have more similarity with the involute splines but the difference lies at the whole depth of the spline. Both the involute splines and gears are manufactured in the same machine but the height of the teeth (addendum and dedendum) is larger for gears compared to the involute splines.

1.6 Spline Tooth Structure Design and Advantages

There are two standards are used for designing the spline geometry which is based on the inch and metric module systems [4]. Inch module systems are followed by the American Standards whereas Metric module is based on ISO standards. The difference between this two standards lies on the symbols that are used to specify dimension and angles. Also, the two systems do not allow the interchangeability of parts. Apart from the international standards, company standards are also available nowadays and it has slight differences in the tolerance value compared to the international standards.

On comparing with the key shaft and slot system, Splines structure provides more advantages. Fatigue life of the shaft gets decreased when the external keyed shaft is subjected to a very high-stress concentration at the root of the key. The slotted shaft which is made to accept the key is weakened significantly. In the case of splines, the load namely bending and torsion distributed on the several teeth and helps to attain the greater strength than keyed connection. Each tooth of the spline shaft acts as a key.

The basic factor such as diametral pitch (P), module (m), Pitch diameter (D), the number of teeth (N), pressure angle, tooth thickness (t) and circular pitch (C) determines the interlocking of the

tooth in the shaft and hub connection. Apart from that, other dimensions such as Major Diameter, Minor diameter and Base diameter are the necessary parameter which determines the shaft shape and addendum & dedendum values. The size of the tooth or the basic space width and the circular pitch is determined by the diametral pitch or by the module. Diametral pitch(P) is the number of spline teeth per inch of pitch diameter [1]. With the number of teeth, it is the major factor to fix the pitch diameter (D) of the shaft.

1.6.1 Spline Teeth Engagement

The typical spline teeth engagement of the involute spline is shown in the figure.

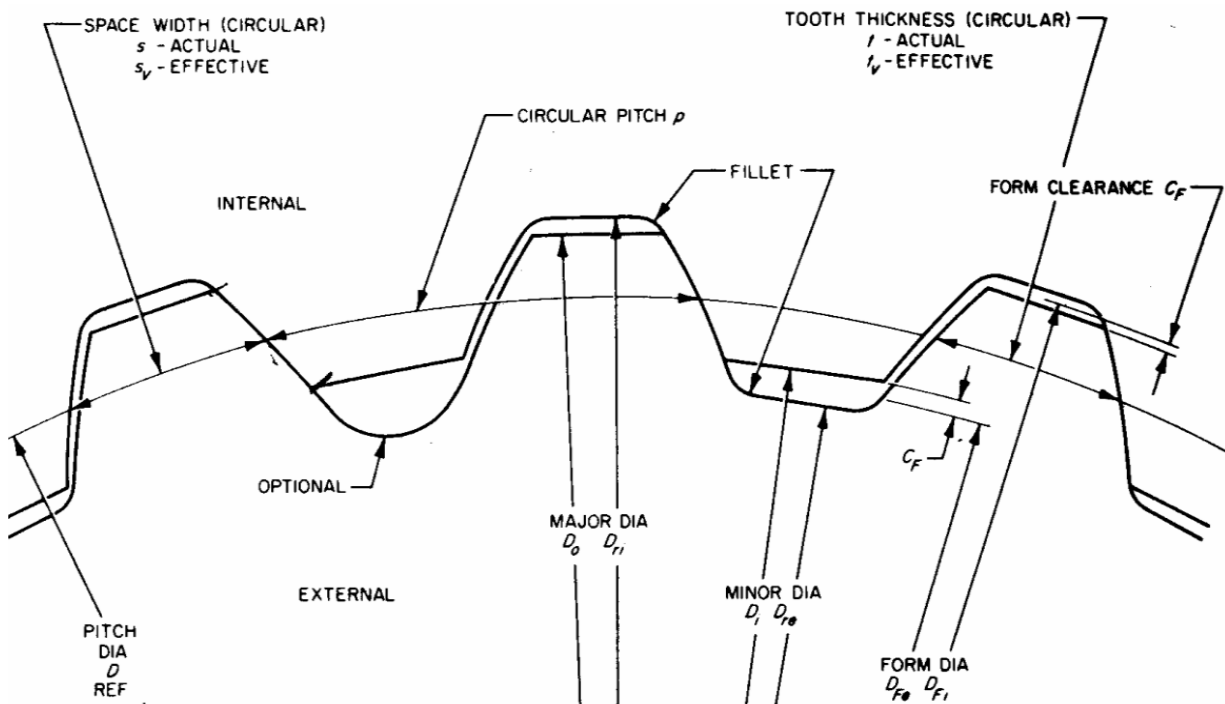


Figure 12: Spline Terms, Symbols, and Drawing Data, 30-Degree Pressure Angle, Flat Root Side Fit ANSI B92.1-1970, R1993 [1]

The teeth of the external splines are projecting outwards. The major diameter refers to the tip of the spline teeth and the minor diameter of the root of the spline. But in the case of internal spline teeth, the teeth of the splines are facing inward. The major diameter refers to the root of the teeth and the minor diameter of the tip of the spline.

1.7 Manufacturing

There are various types of shaft connections are in use for fixed and sliding applications. Among these connections are the ordinary key and keyway, multiple keys and keyways, three and four-lobed polygon shaft and hub connections, and involute splines of both inch dimension and metric module sizes [4]. The major benefit of using involute splines for interference as well as sliding connections is that they are very stronger than other connection types except polygon shaped members. The manufacturing equipment for involute splines is same as that of the gears. External splines are commonly manufactured by the technique called hobbing. Hobbing is a technique which uses a rotating tool called a hob to cut the grooves into a solid shaft. Hob or cutting tool is of various designs which can be used to cut the desired involute splines. Apart from hobbing, the broaching technique is also used to manufacture external and internal spline teeth.

Based on the external spline tooth thickness and the number of teeth, the internal splines are manufactured with the space width. Machining of grooves parallel to the shaft axis can be done based on the internal diameter of the shaft. The external splined shaft which has the similar grooves made up the inner part i.e., the external splined shaft is fitted inside the internal splined housing. Lubricants are resin coating is provided to avoid the wear and to provide the frictional resistance to the shaft. Since mating members are considered for the analysis, the splines are referred to as ‘closed’.

Based on the Japanese Unexamined Patent Publication No.2005-153677(3), the tooth of the telescopic splined shaft is surface hardened by the shot peening method which forms a large number of alcoves. It serves as a reservoir for grease. In the later development, Resin coating is provided on the core root portion of the inner shaft which gives the better results on durability. Backlash in the early stage of use is reduced and the vibration of the shaft gets suppressed [3].

1.8 Tooth Deviation

Even though proper tolerance is provided, it is difficult to get the perfect spline after machining and heat treatment [2]. It leads to the formation of some deviations. The most important deviations occur in spline teeth manufacturing are the deviations of profile, deviation of pitch and lead deviation. Normally the deviation of the involute splines changes the connection of the fit and also the maximum material condition.

For proper fitting of the assembly, there are two different dimensions considered namely actual and the effective thickness of the tooth. Actual thickness is the value of the circular tooth thickness value which is designated as S_{max} and S_{min} . The effective thickness of the tooth is the value of the circular space width on the pitch diameter of the internal spline teeth which is designated as S_{vmax} and S_{vmin} [2]. The difference between them is that the actual dimensions are used to determine the strength of the spline tooth and the effective dimensions are used to control the clearance value [7].

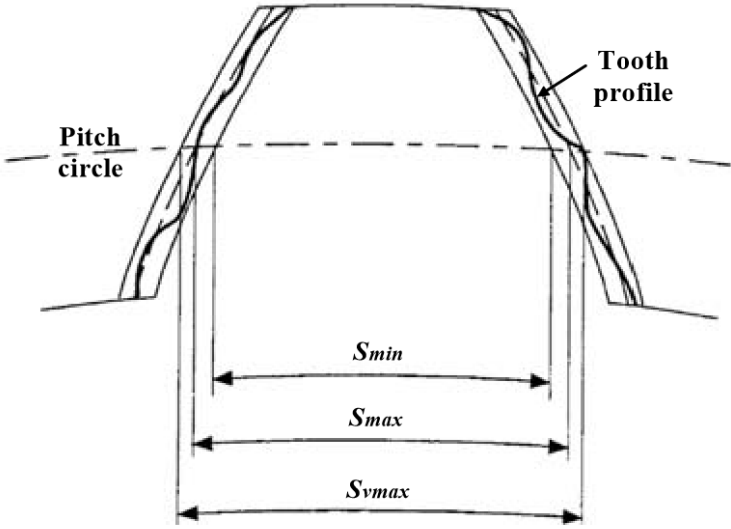


Figure 13: Actual and effective tooth thickness [2]

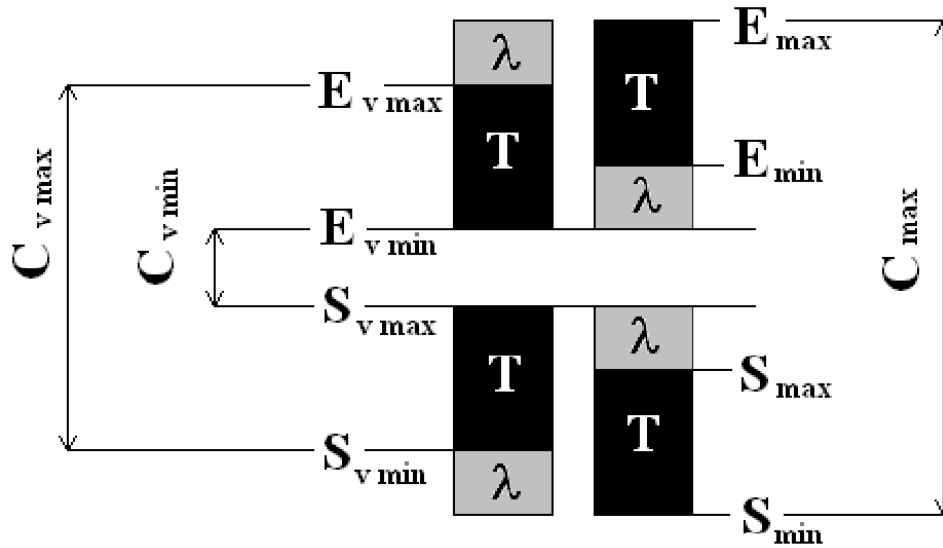


Figure 14: Tolerance zones for the tooth thickness and the space width

T – machining tolerance, λ – deviation allowance, $(T+\lambda)$ – total tolerance, $S(E)_{\max}(\min)$ – maximum (minimum) actual tooth thickness (space width), $S(E)_{v\max}(v\min)$ – maximum (minimum) effective tooth thickness (space width), $c_{v\min}(v\max)$ – minimum (maximum) effective clearance, c_{\max} – maximum clearance [2]

The fit of the internal and the external parts which act as a mating member is defined by the effective clearance. It is the value of the difference between the effective tooth thickness and the effective space width. The assembly is controlled by the two types of fit. The first type of fit has minimum space width with minimum clearance value and the maximum tooth thickness whereas the second type of fit has maximum space width with maximum clearance and minimum tooth thickness.

This effective variation called deviation allowance λ is the determining factor of fit of the assembly. It depends on the total pitch deviation F_p , total lead deviation F_β and total profile deviation F_α . The deviation allowance is given by the following equation [1]:

$$\lambda = 0.6 \sqrt{F_p^2 + F_\alpha^2 + F_\beta^2} \quad (1.21)$$

From the equation 1.21, it is noted that the deviation allowance is the value of sixty percentage of the sum of the form deviations.

From the standard [2], the formulas to find the individual form deviation is given in the table.

Table 2:Form deviation [2]

| Spline Tolerance Class | Total pitch deviation $F_p (\mu m)$ | Total profile deviation $F_\alpha (\mu m)$ | Total lead deviation $F_\beta (\mu m)$ |
|---|---|---|---|
| 4 | $2.5 \cdot \sqrt{m \cdot z \cdot \pi/2} \div 6.3$ | $1.6 \cdot (m + 0.0125 \cdot m \cdot z) + 10$ | $0.8 \cdot \sqrt{L} + 4$ |
| 5 | $3.55 \cdot \sqrt{m \cdot z \cdot \pi/2} \div 9$ | $2.5 \cdot (m + 0.0125 \cdot m \cdot z) + 16$ | $\sqrt{L} + 5$ |
| 6 | $5 \cdot \sqrt{m \cdot z \cdot \pi/2} \div 12.5$ | $4 \cdot (m + 0.0125 \cdot m \cdot z) + 25$ | $1.25 \cdot \sqrt{L} + 6.3$ |
| 7 | $7.1 \cdot \sqrt{m \cdot z \cdot \pi/2} \div 18$ | $6.3 \cdot (m + 0.0125 \cdot m \cdot z) + 40$ | $2 \cdot \sqrt{L} + 10$ |
| Where: m-module, z-number of teeth, L-the spline length | | | |

1.9 Spline Teeth and Applications

The shaft with splined joints is having a series of parallel keys formed integrally with the shaft and the joints are mating with the corresponding grooves cut in a hub or fitting [1]. This kind of shafts provides a better torque-transmitting capacity. Splined shafts are most generally used in the following three types of applications [1].

1. Used in the coupling mechanism where relatively high torques are to be transmitted with negligible slippage.
2. Used for transmitting power to fixed or sliding rotating members like gears, pulleys etc.,
3. Used in the jointed parts for easy removal for changing angular position and indexing.

1.10 Wear in the spline shaft

Wear resistance is the important factor which decides the reliability of the spline shaft. The possible wear which will happen in the spline shaft is the fretting wear, fretting corrosion wear and abrasion wear [17]. Fretting is a kind of wear process which occurs mainly at the contact surfaces of the mating members when it is subjected to external load or force which cause sliding.

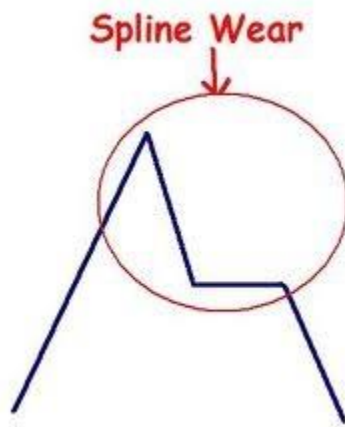


Figure 15: Wear Pattern [18]

The wear pattern which is commonly occurring in the splines is represented in the figure and is called as “the mountain effect” [18]. The worn spline teeth have a sharp peak at one side which is shown in the figure. Under external load, spline tooth started to slide back and forth against each other. The wear happened in the splines is less when proper lubrication is available. In the case of insufficient lubrication at the mating member, the metal to metal contact is high and the occurrence of wear at the sliding part is increasing drastically.

1.11 Importance of Hardness in the Splined Shaft

Based on the study conducted on the splined axial shaft, I.Borshum, Z.Borshum and F.Khan [13] has selected six different spline geometries and seven different hardness profiles including non-hardened and through-hardened shafts. Based on the result made by finite element modelling, torque causing yielding of induction hardened splined shafts is strongly dependent on the hardness depth and the geometry of the spline teeth. They have concluded that the torsional strength has been improved if the shaft is hardened to half of the radius and have no influence if the hardening is increasing more than half of the radius. Also, increasing the number of teeth Z , which corresponds to increase the dedendum radius “ r_d ” and keeping the addendum radius constant, increase the torsional strength of the shaft. The number of spline teeth will have an impact on the level of static torque [13].

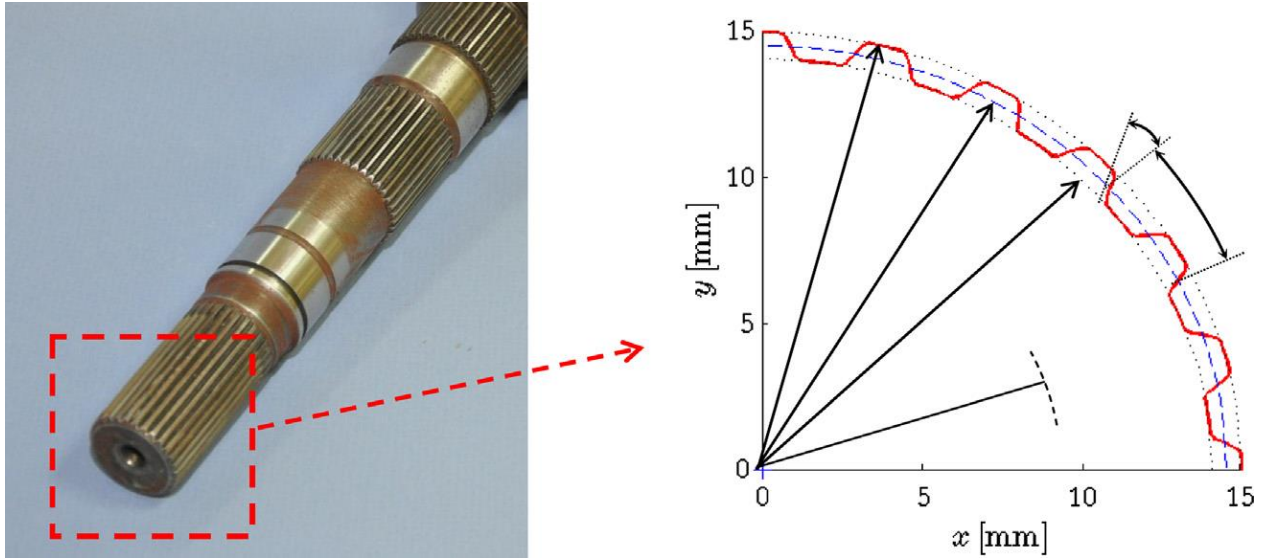


Figure 16: Spline tooth profile of the axial shaft [13]

They found that increasing the hardness also increase the wear resistance of the splined shaft and the torsional strength of the shaft. They also concluded that increasing the pressure angle won't provide many benefits for increasing the strength.

2. CHEMICAL ANALYSIS

2.1 Material in Use

The telescopic splined steel shafts, that is in real time use has been chosen and chemical analysis has been made to find the exact material composition used by the manufacturers. The instrument used for chemical analysis is Brucker Q4 Tasman.

2.1.1 Brucker Q4Tasman

Brucker Q4 TASMANTM is a well-developed tool to perform metal analysis and to find the chemical composition. It works based on optical emission spectrometer. It provides advanced and reliable results on a quicker basis. It provides dedicated solutions for metal analysis.

2.1.2 Spectroscopic Analysis

In order to check the chemical composition, the sample alloy was subjected to spectroscopic analysis. The experiment was conducted using a Q4 Tasman optical emission spectrometer. The laboratory of Lithuanian energy institute offers a chemical analysis expertise for determining material composition and the element analysis. The analysis was done under the supervision of the experts who has already performed different kinds of metals analysis. It uses the technique which includes the sparking OES database. Bulk analysis of various materials and alloys can be done argon gas atmosphere.



Figure 17: Brucker Q4Tasman Apparatus Setup

2.1.3 Sample for Chemical Analysis

For sample making, the specimen has been cut and the sample should have at least 1 flat surface, 20 mm or larger.



Figure 18: Sample Prepared for Chemical Analysis

2.2 Steps Involved in Analysis

The following steps are involved in performing chemical analysis of the shaft which has taken for study.

1. The prepared sample is placed onto the arrangement called spark stand plate and it is covered fully. The prepared sample is placed at least one millimetre over the edge of the opening. The spark spots are located closer to the outer edge of the sample.
2. The sample is fixed with the help of sample clamp and the safety circuit is closed. It is necessary to ensure the sample position.
3. Once the sample position is checked, the start button is pressed and the process is started. QMatrix software is used in the instrument used for the study.
4. Once the process gets started, sounds of the different sparking sequence are generated and the sample identification is entered.
5. Once the analysis gets finished, the measurement results are displayed on the screen.
6. Later, the sample is removed and the electrode is cleaned with the wire brush.
7. Again, the process is repeated by placing the sample and the electrode is faced at the different position of the sample.

8. In this present research study, the experimental analysis is repeated for four times and the results are compared.

9. Once the analysis is finished, the results will be saved and exported as a report

From the analysis, the material composition has been shown in the table.

Table 3:Sample T-Fe

| Sample | C % | Si % | Mn % | P % | S % | Cr % | Mo % | Ni % | Cu % |
|--------|-------|-------|-------|--------|--------|-------|-------|-------|-------|
| | 0.353 | 0.199 | 0.768 | 0.0170 | 0.0143 | 0.115 | 0.007 | 0.023 | 0.015 |
| Al % | Co % | Nb % | Pb % | Sn % | Ti % | V % | W % | Zr % | |
| | 0.052 | 0.003 | 0.003 | 0.014 | 0.002 | 0.001 | 0.002 | 0.014 | 0.001 |

After the analysis is finished, the average of the experimental results is noted and it was compared with the standard values. It was verified that the chemical constituents of the sample shown in the above table are validated with ASM data sheet specifications.

Based on the chemical analysis results, the material grade used in the splined shaft which is used for this study is SAE 4140 Steel.

2.3 Metallurgical Characterization

The chemical composition is found by conducting the test and analysis. It is used for finding the grade of the steel, and the standard mechanical properties and the metallurgical conditions of the shaft are assumed which is helpful for the comparison with the design requirements.

2.3.1 Materials

By considering the importance of material properties, the materials with low frictional coefficient and weight will have a greater effect on improving the performance. Similar materials in contact will have a greater coefficient of friction than the component with different materials [15]. In this paper, the material which is taken into the account for the analysis is SAE 4140(42CrMoS4) [13].

Table 4: Material Properties

| Material grade | Elastic modulus E N/m ² | Hardness(HB) | Yield strength R_e N/mm ² | Tensile strength R_m N/mm ² | Poisson's ratio |
|--------------------------|---|--------------|---|--|-----------------|
| SAE 4140(fully annealed) | 2.05×10^{11} | 197 | 373.02 | 684.07 | 0.29 |

The properties provided in the table is based on the data of heat treatment done on the SAE 4140 under fully annealed condition [20].

3. DESIGN METHODOLOGY

The design which was taken into consideration was done with the model of the involute splined shaft with the actual dimensions. Since the design of involute splines and their manufacture requires considerable knowledge, not only of the basic properties of the involute profile but also of various other elements which affect the spline fit and the sometimes complex principles underlying manufacturing and checking equipment, the question is frequently raised as to why the involute profile is given preference in designing splines over the seemingly simpler straight sided tooth profile [16]. In case of the splined shaft in use, the contact surface of teeth side of the shaft is important for the fitting and it is desirable to check the torsional stiffness of the straight-sided teeth compared to the involute teeth.

In this research study, the design approach conducted is based on the closer inspection made on the shaft which is facing frequent failures. To understand the position of the mating member inside the spline housing, a piece of the shaft is cut at the place of housing and it is subjected to visual inspection under a microscope. It is used to find the gap between the spline teeth which helps on finalising the tolerance class. The image of the shaft is shown in the figure.



Figure 19: Cross-sectional view of the Spline Shaft

3.1 Pressure Angle Inspection

By doing the closer visual inspection, the spline tooth has more gaps between the internal and the external spline shaft. From the fit class shown in the table, the fit class which matches to the shaft taken into consideration is the locational clearance fit. The locational clearance fit is the fit which provides a snug fit for locating stationary parts but can be freely assembled and disassembled. Also from the image, it is clear that the pressure angle used on the external spline shaft is 45° .

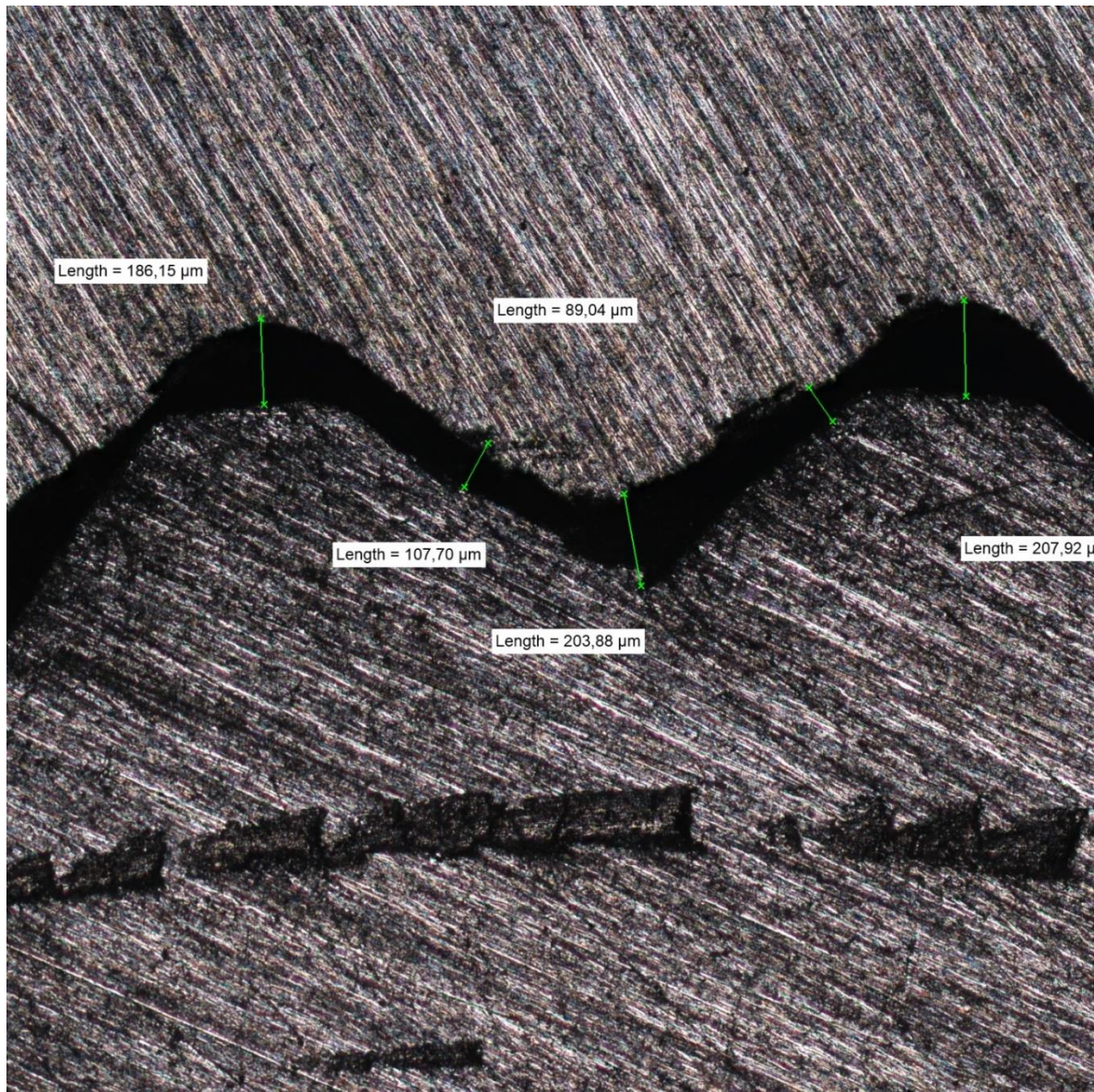


Figure 20: Microscopic view of the mating member of the telescopic spline shaft.

3.2 Influence of design and analysis:

From the inspection made on the figure and the data collected from the experimental model, the pressure angle chose for the model is 45^0 . Based on the pressure angle, the dimensions of the splined shaft are calculated based on the standards [1].

3.3 Experimental Shaft

The model of the shaft which is taken for the research study is designed with the help of Solidworks. It is achieved by importing the image of the portion of the shaft shown in the figure to the Solidworks. The different model of the shaft is designed based on the imported image of the shaft and the iteration has been made to find the dimensions of the shaft. It has been achieved by choosing four teeth of the image and the design is extruded. From the extruded design, the dimension of the teeth, the necessary outer& inner diameter of the internal and external splines is found and tabulated. Following the same principle, different model based on the teeth is made.

Based on the measured outer diameter of the shaft, the scale factor is calculated and all the models are reduced based on the scale factor. From the models, the average value is calculated and the experimental model is designed. The dimension of the model is noted and tabulated.

Table 5:Dimension of the experimental Spline Shaft

| Dimensions | Symbols | Model 1 (mm) | Model 2 (mm) | Model 3 (mm) | Model 4 (mm) | Average (mm) |
|--|----------|-----------------|-----------------|-----------------|-----------------|-----------------|
| Number of Teeth | N | 36 | 36 | 36 | 36 | 36 |
| Pitch Diameter | D | 16.445 | 16.42 | 16.527 | 16.4643 | 16.4431 |
| Pressure Angle | Φ_D | 45^0 | 45^0 | 45^0 | 45^0 | 45^0 |
| Major Diameter(External) | D_o | 16.9667 | 16.62 | 16.95 | 16.84 | 16.8089 |
| Minor Diameter(External) | D_{re} | 15.997 | 15.94 | 16.05 | 15.889 | 15.942 |
| Tooth Thickness (at Pitch Diameter) | T | 0.716 | 0.7 | 0.839 | 0.707 | 0.707667 |

| | | | | | | |
|--------------------------|------------------|---------|-------|--------|---------|----------|
| Whole Depth of the teeth | H | 0.41 | 0.34 | 0.45 | 0.48 | 0.41 |
| Major Diameter(Internal) | D _{ri} | 16.9667 | 16.97 | 16.96 | 16.9667 | 16.9678 |
| Minor Diameter(Internal) | D _i | 16.17 | 16.21 | 16.39 | 15.889 | 16.08967 |
| Space Width | S | 0.9216 | 0.803 | 0.8795 | 0.914 | 0.879533 |
| Whole Depth of the teeth | H | 0.33 | 0.38 | 0.28 | 0.36 | 0.4 |
| Outer Housing Dia | D _{out} | 21.73 | 22.17 | 22.77 | 21.9 | 21.93333 |

3.4 Calculation Based on the Standards

The following procedure is used for calculating the dimensions:

1. Measure the external spline diameter of the shaft using the Vernier Caliper. Based on the reading, the outer diameter of the shaft is calculated.
2. Once the outer diameter and the number of teeth “N” are known, the diametral pitch “P” of the spline is calculated by the following formula.

$$\text{Diametral Pitch, } P = \frac{\text{Add 2 teeth} + N}{\text{Outer Diameter}} \quad (3.1)$$

3. Based on the calculated diametral pitch, the module “M” of the teeth which are used to predict the teeth arrangement is calculated.

$$\text{Module, } M = \frac{25.4}{P} \quad (3.2)$$

4. Pitch diameter “D’ is the diameter in which the pitch circle is constructed. It is a reference circle in which the transverse of spline tooth is constructed. Pitch diameter is given by the following equation.

$$\text{Pitch Diameter, } D = N/P \quad (3.3)$$

5. Stub pitch “ P_s ” is given by the twice of the diametral pitch.

$$\text{Stub Pitch, } P_s = 2P \quad (3.4)$$

6. The involute spline tooth profile is constructed on the base circle and the diameter of the base circle is called base diameter “ D_p ”. Base diameter is given by the following equation.

$$\text{Base Diameter, } D_p = D \cos \phi_D \quad (3.5)$$

7. The major diameter of the internal spline shaft “ D_{ri} ” is the diameter in which the root of the spline teeth is located. The major diameter based on the pressure angle 45° which matches with the model taken for the study is given by the following equation with fillet root side.

$$\text{For } 45^\circ \text{ Pressure angle, } D_{ri} = N + 1.4/D \quad (3.6)$$

8. The minor diameter of the internal spline shaft “ D_i ” is the diameter in which the top of the spline teeth is located and is projecting inwards. The following equation is used to calculate the minor diameter of the internal spline shaft with fillet root side.

$$\text{For } 45^\circ \text{ Pressure angle, } D_i = N - 0.6/D \quad (3.7)$$

9. The major diameter of the external spline shaft “ D_o ” is the diameter in which the top of the spline teeth is located and is projecting outwards. The following equation is used to calculate the major diameter of the external spline shaft with fillet root side.

$$\text{For } 45^0 \text{ Pressure angle, } D_o = N + 1/D \quad (3.8)$$

10. The root of the spline tooth is located to the minor diameter of the external spline shaft “ D_{re} “. The equation of the minor diameter with fillet root side is given by,

$$\text{For } 45^0 \text{ Pressure angle, } D_{re} = N - 1/D \quad (3.9)$$

11. Once the dimensions are calculated the tooth profile is created on the internal and external spline shaft. The thickness of the tooth “ t ” created on the external spline shaft is given by,

$$\text{Tooth Thickness, } t = \pi/2P = 0.5\pi M \quad (3.10)$$

Space width “ S ” is thickness of the gap in the pitch diameter of the internal spline shaft and is given by,

$$\text{Space Width, } s = t + (T + \lambda) \quad (3.11)$$

Where “ T ” is the machining tolerance and “ λ ” is the Variation tolerance.

12. The tolerance class which is chosen from the ISO standard [1] is Class 7.

$$\text{For spline Tolerance class 7, } T+\lambda = 40i^* + 160i^{**} \quad (3.12)$$

Where $i^* = 0.001(0.45\sqrt[3]{D} + 0.001D)$ for $D \leq 500mm$

$$i^{**} = 0.001(0.45\sqrt[3]{S_{bSC}} + 0.001S_{bSC}), \quad S_{bSC} = t$$

3.5 Mathematical Design Calculations

a) Diametral Pitch:

$$P = 36 + 2/0.685"$$
$$= 55.47 \text{ (No Dimension)}$$

b) Module:

$$M = 25.4/55.47$$
$$= 0.457 \text{ (No Dimensions)}$$

c) Pitch Diameter

$$D = 36/55.47$$
$$= 0.649'' = 16.49 \text{ mm}$$

d) Base Diameter

$$= 0.649'' \times \cos 45^\circ$$
$$= 0.459'' = 11.66 \text{ mm}$$

From the Figure, It is found that the fillet root side is found at the root side. So the diameter is calculated with the equation for fillet root side from the standard.

3.5.1 Internal Spline shaft

e) Major Internal Diameter

$$D_{ri} = 36 + 1.4/55.47$$
$$= 0.6744'' = 17.13 \text{ mm}$$

f) Minor Internal Diameter

$$D_i = 36 - 0.6/55.47$$
$$= 0.6382'' = 16.21 \text{ mm}$$

3.5.2 External Spline shaft

g) Major External Diameter

$$\begin{aligned}D_o &= 36 + 1/55.47 \\ &= 0.6672'' = 16.949\text{mm}\end{aligned}$$

h) Minor External Diameter

$$\begin{aligned}D_{re} &= 36 - 1/55.47 \\ &= 0.631'' = 16.03\text{mm}\end{aligned}$$

i) Tooth Thickness

$$\begin{aligned}t &= 0.5\pi \times 0.4535 \\ &= 0.712\text{mm}\end{aligned}$$

j) Tolerance

$$\begin{aligned}i^* &= 0.001(0.45\sqrt[3]{16.49} + 0.001 \times 16.49) \\ &= 0.0016189\text{mm} \\ i^{**} &= 0.001(0.45\sqrt[3]{0.712} + 0.001 \times 0.712) \\ &= 0.000401706\text{mm} \\ T+\lambda &= 40 \times 0.0016189 + 160 \times 0.000401706 \\ &= 0.129\text{mm}\end{aligned}$$

k) Space Width

$$\begin{aligned}S &= 0.712 + 0.129 \\ &= 0.841 \text{ mm}\end{aligned}$$

l) Form Clearance

$$cF = 0.001 \times 0.649$$

$$= 0.000649'' = 0.016\text{mm}$$

The dimensions of the shaft which was selected are calculated and the design has been made by using Solidworks.

Table 6: Splined Shaft Dimensions

| Dimensions | Symbols | Dimensions (ANSI) | Dimensions (ISO) |
|-------------------------------------|-----------------|-------------------|------------------|
| Diametral Pitch | P | 56 (rounded off) | 2 (rounded off) |
| Number of Teeth | N | 36 | 36 |
| Module | M | 0.4535 | 12 |
| Stub Pitch | P _s | 112 | 4 |
| Pitch Number | | 56/112 | 2/4 |
| Pitch Diameter | D | 0.649'' | 16.49mm |
| Pressure Angle | Φ _D | 45 ⁰ | 45 ⁰ |
| Base Diameter | D _b | 0.459'' | 11.66mm |
| Tooth Thickness (at Pitch Diameter) | T | 0.02803'' | 0.712mm |
| Major Diameter(External) | D _o | 0.6672'' | 16.949mm |
| Minor Diameter(External) | D _{re} | 0.6311'' | 16.03mm |
| Major Diameter(Internal) | D _{ri} | 0.6744'' | 17.13mm |
| Minor Diameter(Internal) | D _i | 0.6384'' | 16.216mm |

| | | | |
|---------------------------|------------------|-----------|--------------|
| Space Width | S | 0.03311" | 0.841mm |
| Outer Housing Diameter | D _{out} | 0.8661 | 22 (Assumed) |
| Clearance Factor | cF | 0.000649" | 0.016 |

Based on the calculated tolerance value of table 3.1 and the experimental tolerance value of table 2 provided to the space width, the fit class value which is chosen for the model is H14/h13. In the fit class, H refers to the space width modifier values and h refers to the tooth thickness size modifier.

4. DESIGN IMPROVEMENT

4.1 Improvement based on Module

In the first case, the improved model is developed by providing concentration on the number of teeth and the thickness of the teeth. From the equation, it is found that the number of teeth and the thickness of the teeth at the pitch diameter are inversely proportional to the shear stress at the root of the teeth.

From the calculation made, the module of the real-time shaft noted is 0.4535. Based on the module, four modules are chosen which has different tooth thickness and the number of teeth. The assumption is made on the whole depth, addendum and dedendum values of teeth, as it is not as same as that of the gear tooth. The other dimensions to design the shaft is same as that of the calculated model. The tolerance value under class 7 is calculated based on the standards [1]. The module and the dimensions are tabulated below.

Table 7: Dimensions based on the Module

| Module “M” | Diametral Pitch “P” | Tooth Thickness “t” (mm) | T+λ (mm) | Space Width “S” (mm) | Number of teeth |
|------------|------------------------|--------------------------------|----------|----------------------------|--------------------|
| 0.3 | 85 | 0.471 | 0.1208 | 0.6 | 50 |
| 0.4 | 64 | 0.6283 | 0.202 | 0.8303 | 41 |
| 0.75 | 34 | 1.178 | 0.141 | 1.319 | 22 |
| 1 | 25.4 | 1.57 | 0.14873 | 1.71873 | 16 |
| 1.25 | 20 | 1.963 | 0.1553 | 2.1184 | 13 |

4.2 Improvement based on the Fit Tolerance

Based on the tolerance class 7, five different models are created by changing the tolerance value of the shaft and the rest of the dimensions are same.

Using the fit class H14/h13, the following five models are designed to check the influence of tolerance class.

- Maximum clearance on both internal and external spline tooth
- Minimum clearance on both internal and external spline tooth
- Average clearance on both internal and external spline tooth
- Maximum tolerance value for internal spline tooth and minimum tolerance value for external spline tooth
- Minimum tolerance value for internal spline tooth and maximum tolerance value for external spline tooth

The tooth thickness and the space width values of the different shaft based on the fit class are tabulated below.

Table 8: Dimensions based on the tolerance variations

| Model | Tooth Thickness “t” (mm) | Space Width “S” (mm) |
|---|--------------------------|----------------------|
| Maximum Tolerance | 0.712 | 0.962 |
| Minimum Tolerance | 0.572 | 0.712 |
| Average Tolerance or Middle-Value Tolerance | 0.642 | 0.832 |
| Maximum – Minimum | 0.572 | 0.962 |
| Minimum – Maximum | 0.712 | 0.712 |

4.3 Improvement based on the Tooth Shape

Based on the shape, three models namely involute shaped teeth and serration-shaped teeth are created.

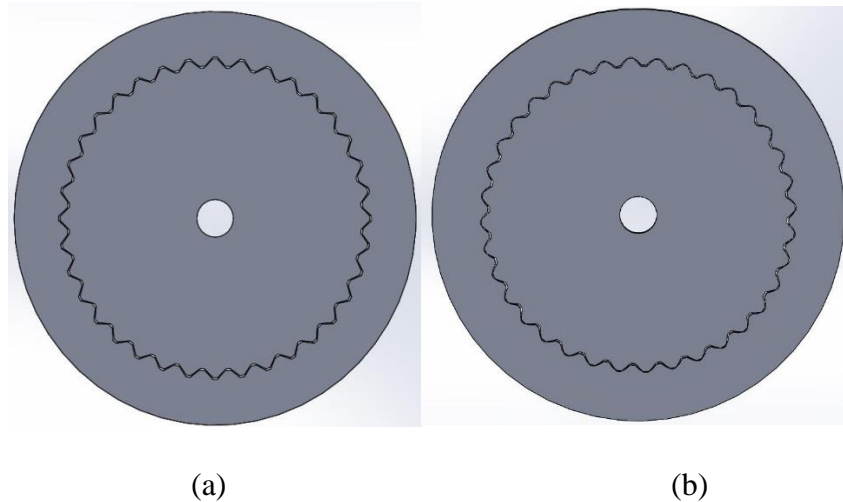


Figure 21: Comparison of Serration Spline (a) and Involute spline (b)

4.4 Improvement based on the Pressure Angle

As the pressure angle at the pitch diameter will generate different shapes, it is important to use different pressure angle to develop an improved model. The different pressure angle will change the shape at the sides of the tooth and it has the impact on the tooth engagement. The change in dimension is not considered as a problem because both the end of the shaft are connected with the help of U-joints. The difference is only of the major & minor diameter of the internal and external diameter of the shaft. The mathematical calculation based on the standards [1] shows that there are no changes made on the pitch diameter, tooth thickness and other important parameters to design the shaft.

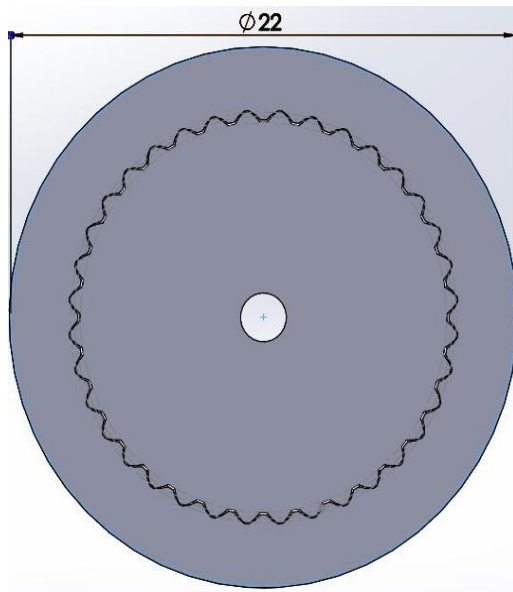
The different pressure angle and the corresponding dimension change based on the pressure angle are tabulated.

Table 9: Dimensions based on the Pressure Angle

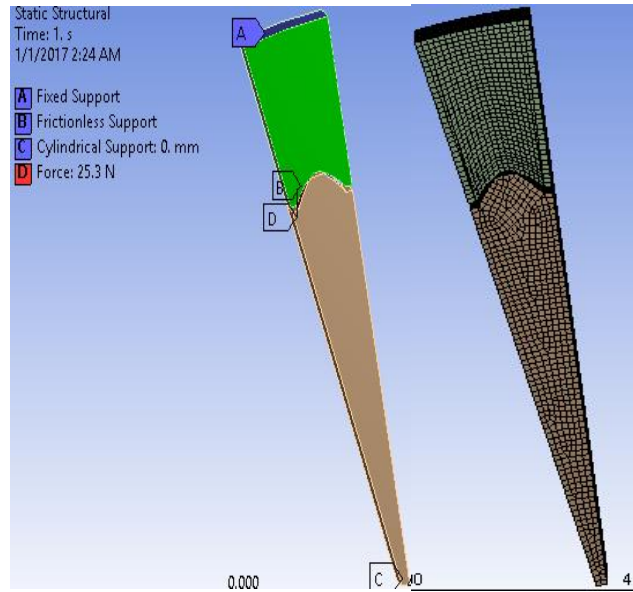
| Dimensions (ISO) | Symbols | 45 ⁰ | 37.5 ⁰ | 30 ⁰ |
|---------------------------------|-----------------|-----------------|-------------------|-----------------|
| Major Diameter External (mm) | D _o | 16.949 | 16.949 | 16.949 |
| Minor Diameter External | D _{re} | 16.03 | 15.89 | 15.57 |
| Major Diameter Internal | D _{ri} | 17.13 | 17.22 | 17.315 |
| Minor Diameter Internal | D _i | 16.216 | 16.12 | 16.03 |

5.FINITE ELEMENT STUDY AND ANALYSIS

The influence of stress – strain state at the mating member of the involute splined joints to the wear resistance and the strength of the joints is investigated based on the finite element analysis method. The 3D geometry of different design of the shaft which is taken into consideration is modelled with the Solidworks. Ansys Workbench tool is used to perform the stress and strain analysis. To make the analysis simple, the model is reduced to the segment representing 1/36 of the entire cross-section and it is utilised together with the boundary condition of Cyclic Symmetry. The sectional part has 1 mm thickness with the additional boundary conditions that created a plain strain analogous as in the 2D plane strain state model. The 3D finite element mesh is shown in the figure. The torque of 10 Nm [19] is applied to the teeth sides of the external splined shaft. As 1/36 of the teeth is taken into consideration, the actual torque applied is 25.3 N of the tangential force. The 2mm diameter hole is created inside the external splined shaft to apply a cylindrical geometry and it is made free along the tangential direction. The fixed geometry is applied to the top of the outer housing and the frictionless geometry is applied to both the sides of the external teeth. A cylindrical coordinate system is generated on the outside of the model that has 11mm radius and the tangential force is applied to the y direction of the cylindrical coordinate system. By using von Mises bilinear isotropic hardening option, A static non-linear solution of the problem was performed for the steel with a tangent modulus of the material $E_T= 572$ MPa.



(a)



(b)

(c)

Figure 22: Geometry of the joint (a); its realisation in ANSYS Workbench with the loads and displacement boundary conditions (b) and the view of the finite element mesh (c).

6.RESULTS

The telescopic splined shaft with various measured dimensions are made with Solidworks and the torsional response has been analysed. It was found that the contact von Mises stress, strain and the deformation are produced on the application of the torque. Every model varies with the result of the application of the torque with the variation provided to the existing model.

6.1 Based on the Module

Changing the module changes the number of teeth and the tangential force acting on the teeth. From the equation, it is evident that the stress developed is inversely proportional to the number of teeth and the tooth thickness and is proved by the results obtained from the finite element analysis. The following table provides the results which are obtained in the analysis results.

Table 10: Stress -Strain results based on the change in module

| Module | Number of teeth | Tangential Force (N) | Max Stress (MPa) | Min Stress (MPa) | Max Strain $\times 10^{-6}$ | Min Strain $\times 10^{-6}$ | Max Deformation (x10-5 mm) | Min Deformation (x10-5 mm) |
|--------|-----------------|----------------------|------------------|------------------|-----------------------------|-----------------------------|----------------------------|----------------------------|
| 1.25 | 13 | 69.93 | 121.57 | 0.43234 | 657.74 | 5.3063 | 33.762 | 0 |
| 1 | 16 | 56.82 | 91.417 | 0.69815 | 493.02 | 5.430 | 23.203 | 0 |
| 0.75 | 22 | 41.32 | 106.26 | 1.2965 | 580.75 | 6.686 | 22.42 | 0 |
| 0.4 | 41 | 22.17 | 76.018 | 0.2086 | 422.12 | 1.4615 | 8.7986 | 0 |
| 0.3 | 50 | 18.18 | 40.344 | 0.17917 | 201.72 | 0.9677 | 3.1493 | 0 |

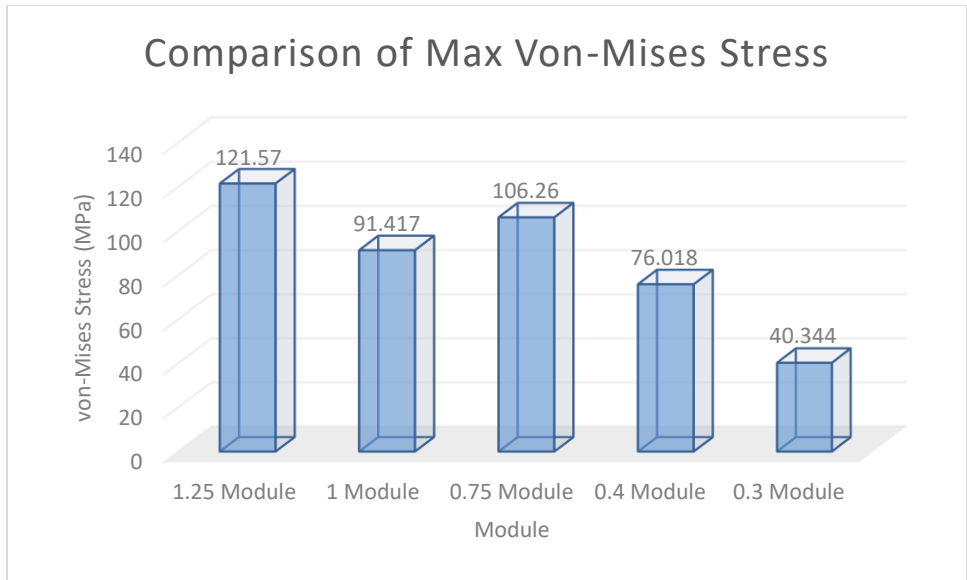


Figure 23: Von-Mises stress developed on the shaft of different modules

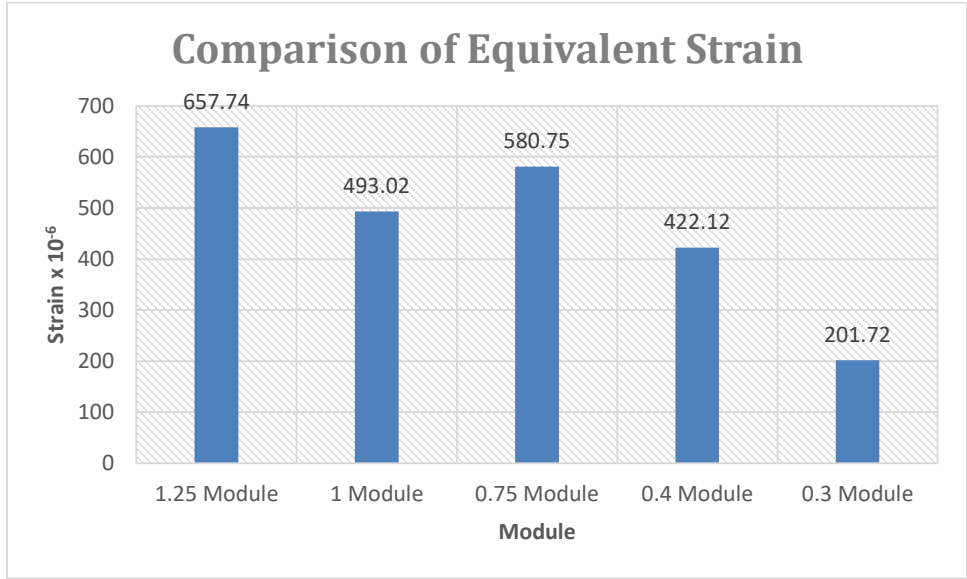


Figure 24: Maximum Equivalent Strain developed on the shaft of different Modules

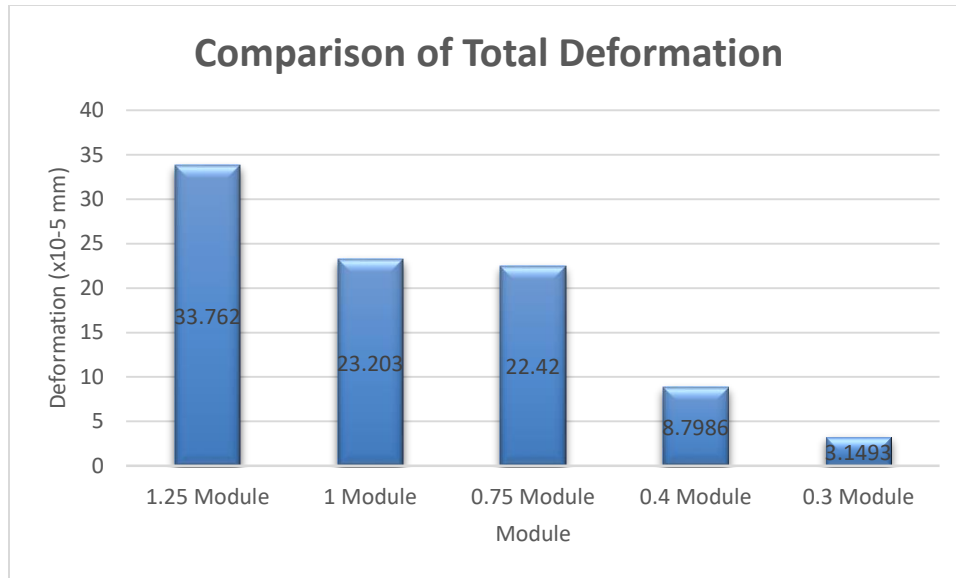


Figure 25: Total Deformation on the shaft of different Modules

From the results obtained, the module of 0.3 with 50 number of teeth shows the improvement in the generation of stress compared to the other module values.

6.2 Based on the Pressure Angle

The importance of the pressure angle in designing the splined shaft is noted with the static analytical results obtained in Ansys Workbench. The results based on changing the pressure angle is tabulated below.

Table 11: Stress-Strain results based on the change in pressure angle

| Pressure Angle (ϕ_D) | Number of teeth | Tangential Force (N) | Max Stress (MPa) | Min Stress (MPa) | Max Strain $\times 10^{-6}$ | Min Strain $\times 10^{-6}$ | Max Deformation (x10-5 mm) | Min Deformation (x10-5 mm) |
|-----------------------------|-----------------|----------------------|------------------|------------------|-----------------------------|-----------------------------|----------------------------|----------------------------|
| 45 ⁰ | 36 | 25.3 | 80.308 | 0.13548 | 470.07 | 0.71 | 9.987 | 0 |
| 37.5 ⁰ | 36 | 25.3 | 41.223 | 0.3838 | 235.44 | 2.277 | 6.0945 | 0 |
| 30 ⁰ | 36 | 25.3 | 31.324 | 0.39161 | 180.62 | 2.592 | 5.31 | 0 |

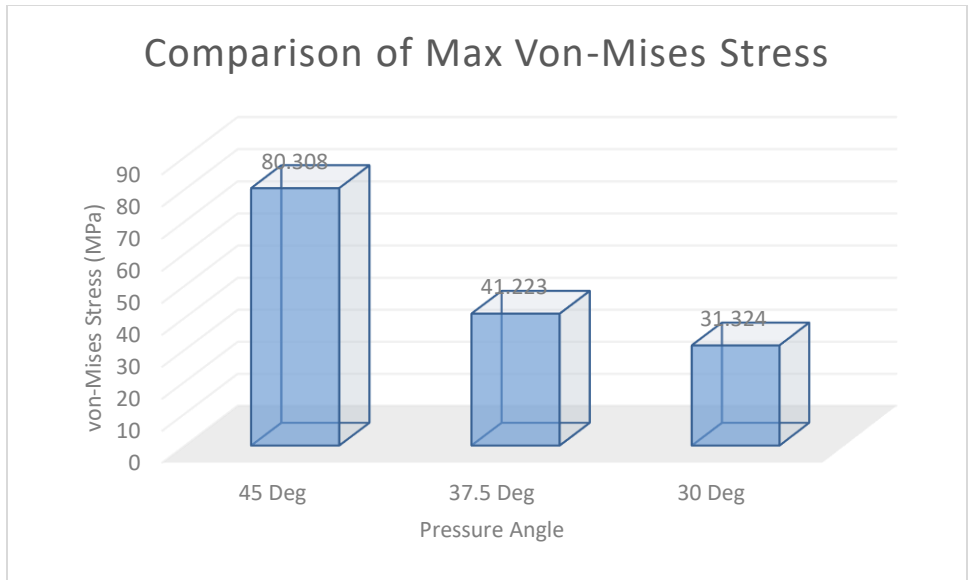


Figure 26: Von-Mises stress developed on the shaft of different pressure angles

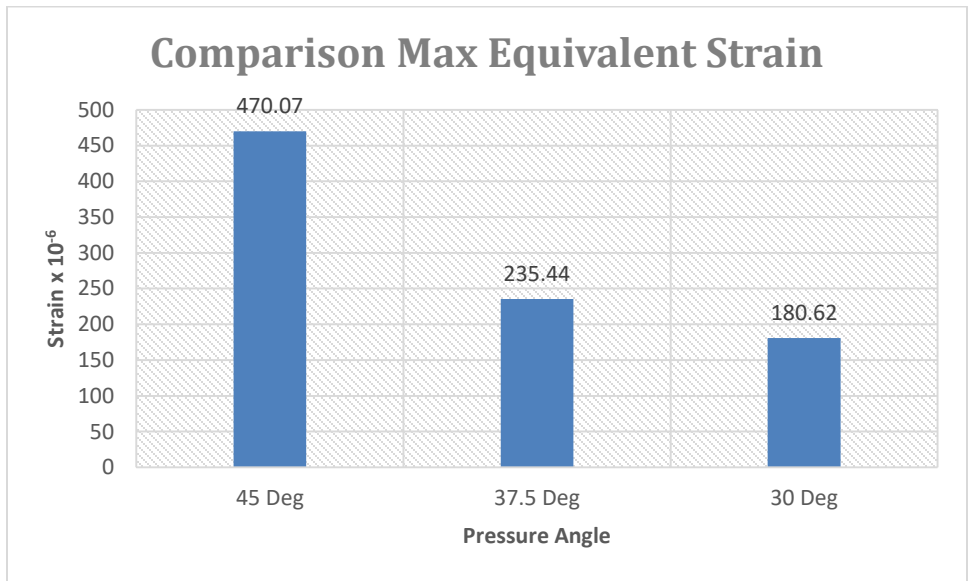


Figure 27: Maximum Equivalent Strain developed on the shaft of different pressure angles

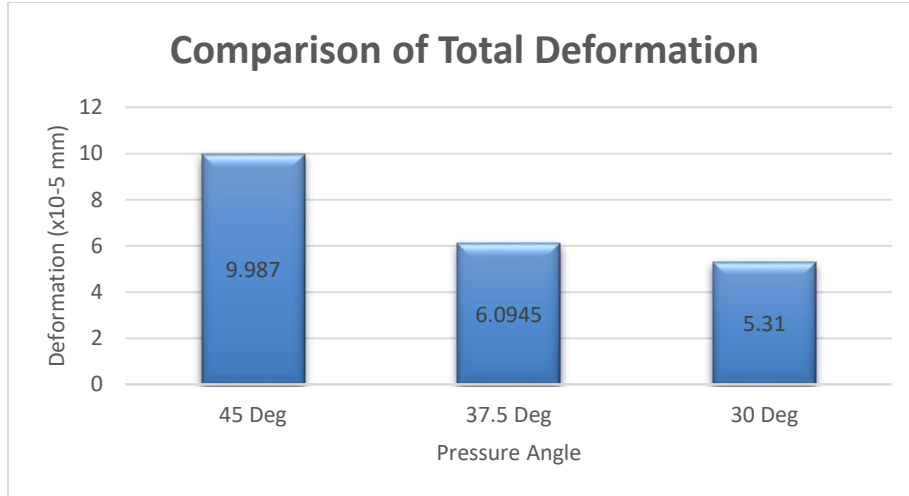


Figure 28: Total Deformation on the shaft of different pressure angles

From the results, it is found that the pressure angle of 30° will provide the improved results which develop less stress on the sides of the teeth compared to the other pressure angles. It is because changing the pressure angle is improving the tooth thickness above the pitch diameter and which can withstand the tangential force acting on it.

6.3 Based on the Tolerance

The stress – strain generation at the sides of the teeth shows drastic change with the change in tolerance class value. The following table provides the analytical results obtained in the Ansys workbench.

Table 12: Stress-Strain analysis results based on the change in tolerance

| Tolerance | Number of teeth | Tangential Force (N) | Max Stress (MPa) | Min Stress (MPa) | Max Strain $\times 10^{-6}$ | Min Strain $\times 10^{-6}$ | Max Deformation (x10-5 mm) | Min Deformation (x10-5 mm) |
|-----------|-----------------|----------------------|------------------|------------------|-----------------------------|-----------------------------|----------------------------|----------------------------|
| Both Max | 36 | 25.3 | 63.387 | 0.29 | 358.44 | 2.4849 | 11.736 | 0 |
| Both Min | 36 | 25.3 | 58.768 | 0.1016 | 344.08 | 0.696 | 24.634 | 0 |
| Average | 36 | 25.3 | 75.188 | 0.2956 | 402.22 | 1.48 | 11.289 | 0 |
| Max-Min | 36 | 25.3 | 73.375 | 0 | 487.89 | 0 | 10.359 | 0 |
| Min-Max | 36 | 25.3 | 85.935 | 0.2766 | 506.22 | 1.9263 | 10.366 | 0 |

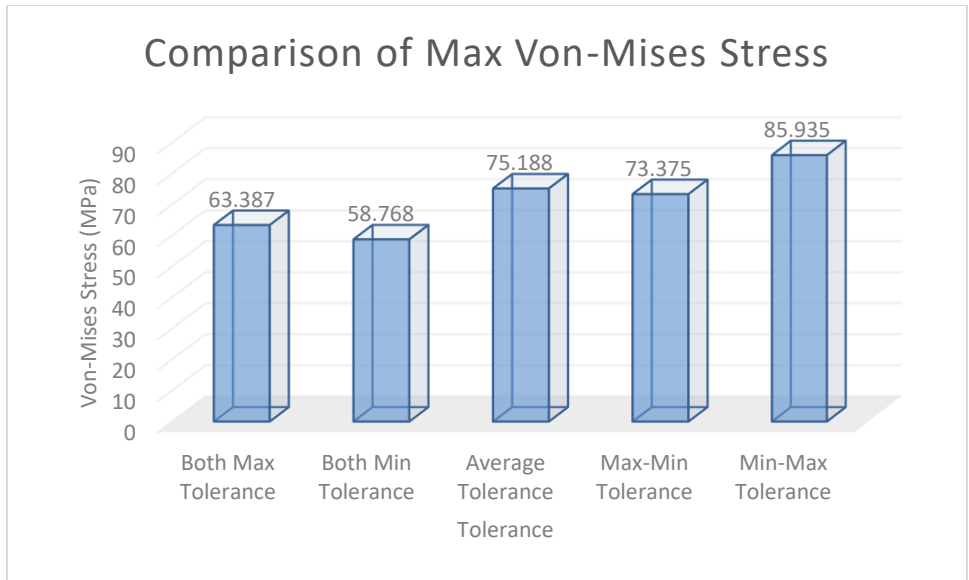


Figure 29: Von-Mises stress developed on the shaft of different Tolerance variations

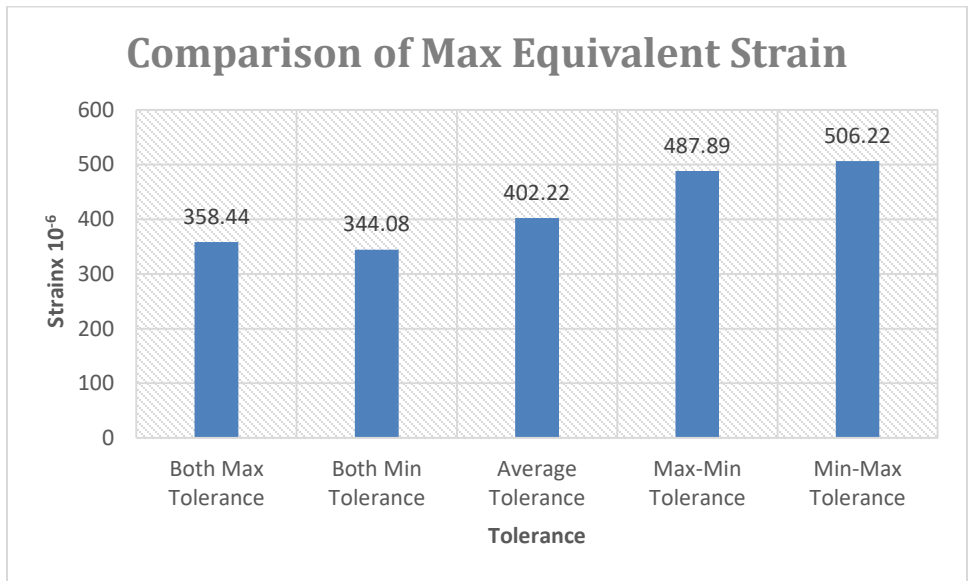


Figure 30: Equivalent Strain developed on the shaft of different pressure angles

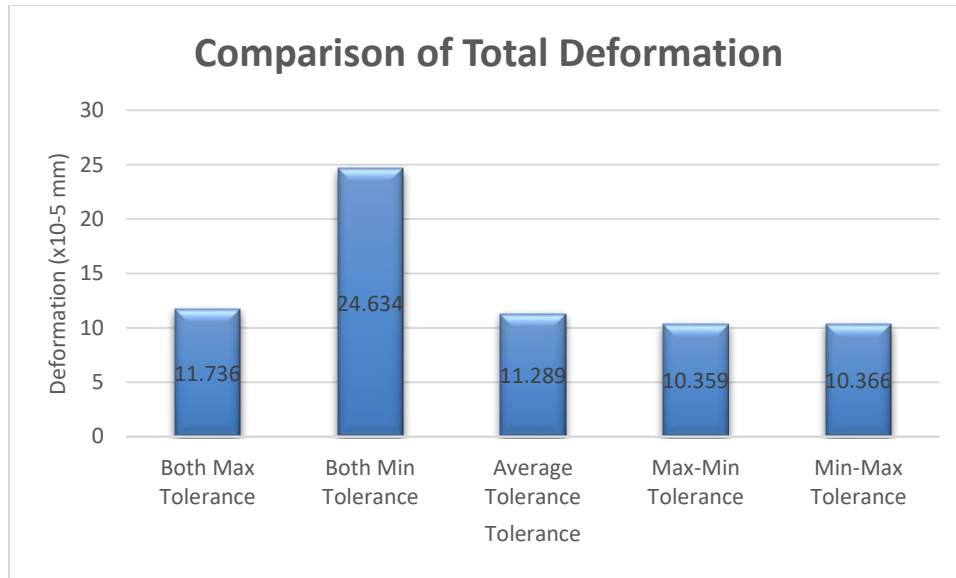


Figure 31: Total deformation on the shaft of different pressure angles

From the results, the tooth with minimum tolerance provides the improved results compared to the other tolerance combinations.

6.4 Based on the shape

The tooth with serration shape provides the improved results compared to the shaft which is designed based on the mathematical calculation. The results are tabulated below.

Table 13: Stress-Strain analysis results based on the shape of the teeth

| Shape | Number of teeth | Tangential Force (N) | Max Stress (MPa) | Min Stress (MPa) | Max Strain $\times 10^{-6}$ | Min Strain $\times 10^{-6}$ | Max Deformation (x10-5 mm) | Min Deformation (x10-5 mm) |
|-----------|-----------------|----------------------|------------------|------------------|-----------------------------|-----------------------------|----------------------------|----------------------------|
| Involute | 36 | 25.3 | 80.308 | 0.13548 | 470.07 | 0.71 | 9.987 | 0 |
| Serration | 36 | 25.3 | 78.722 | 0.1186 | 453.3 | 1.058 | 11.867 | 0 |

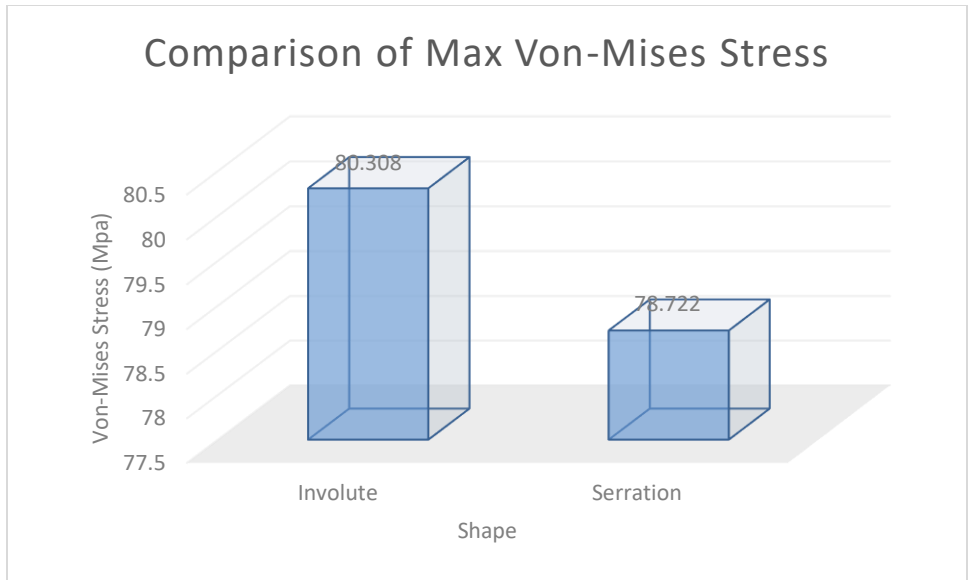


Figure 32: Von-Mises stress developed on the shaft of two different shapes

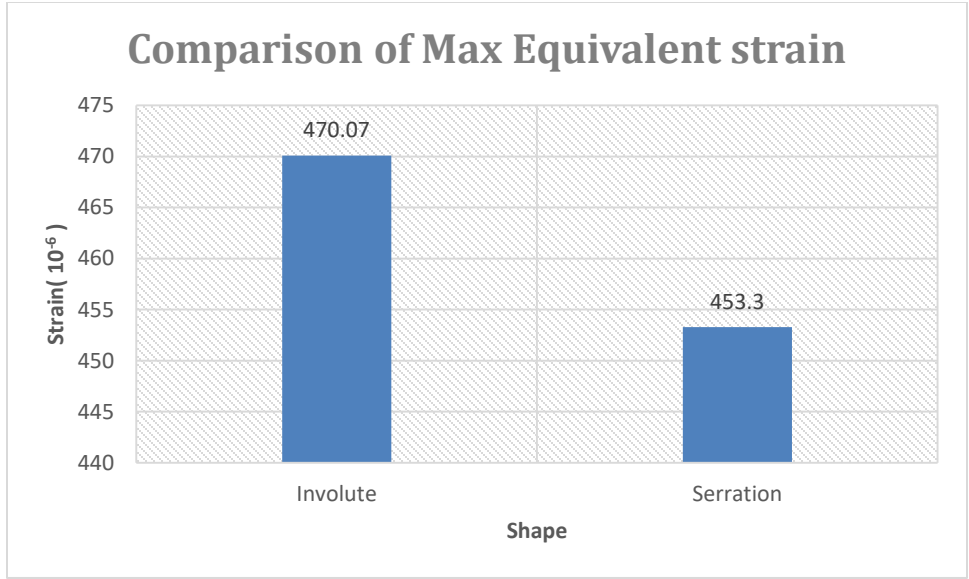


Figure 33: Maximum Equivalent Stress developed on the shaft of two different pressure angles

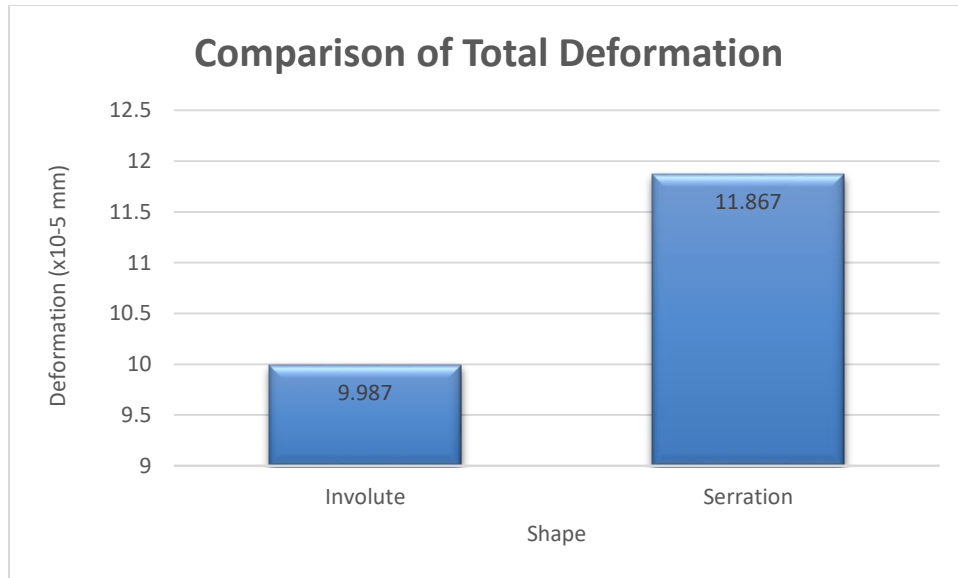


Figure 34: Total Deformation on the shaft of two different pressure angles

6.5 Improved Model

The Static Analysis investigation with the total of 15 models with four different combinations is done with the Ansys Workbench. As the clearance or backlash is the major problem stated in the study, the tolerance value of the experimental model is reduced with the theoretical tolerance. On making analysis, the model with the calculated dimensions doesn't provide the improvement compared to the experimental model. Later the variations are considered and the different model is subjected to analysis. The improvement found in the different combination is provided in the table.

Table 14: Stress-Strain results of the models with improvement

| Model | Max Stress (MPa) | Min Stress (MPa) | Max Strain x 10 ⁻⁶ | Min Strain x 10 ⁻⁶ | Max Deformation (x10 ⁻⁵ mm) | Min Deformation (x10 ⁻⁵ mm) |
|--------------------------------|------------------|------------------|-------------------------------|-------------------------------|--|--|
| Experimental | 45.872 | 0.3216 | 261.66 | 2.3809 | 7.6858 | 0 |
| Calculated (Class 7) | 80.308 | 0.13548 | 470.07 | 0.71 | 9.987 | 0 |
| Module Change | 40.344 | 0.17917 | 201.72 | 0.9677 | 3.1493 | 0 |
| Tolerance - Min | 58.768 | 0.1016 | 344.08 | 0.696 | 24.634 | 0 |
| Shape-Serration | 78.722 | 0.1186 | 453.3 | 1.058 | 11.867 | 0 |
| Pressure Angle-30 ⁰ | 31.324 | 0.3916 | 180.62 | 2.592 | 5.31 | 0 |

From the table 6.5, it is found that the improvement provided on considering the pressure angle 30⁰ is providing better results on static analysis. The generation of stress, strain and the total deformation occur in the improved model is less compared to all the other models of the telescopic splined shaft.

6.6 Comparison of Mises Stress of the Experimental and Improved Model under load

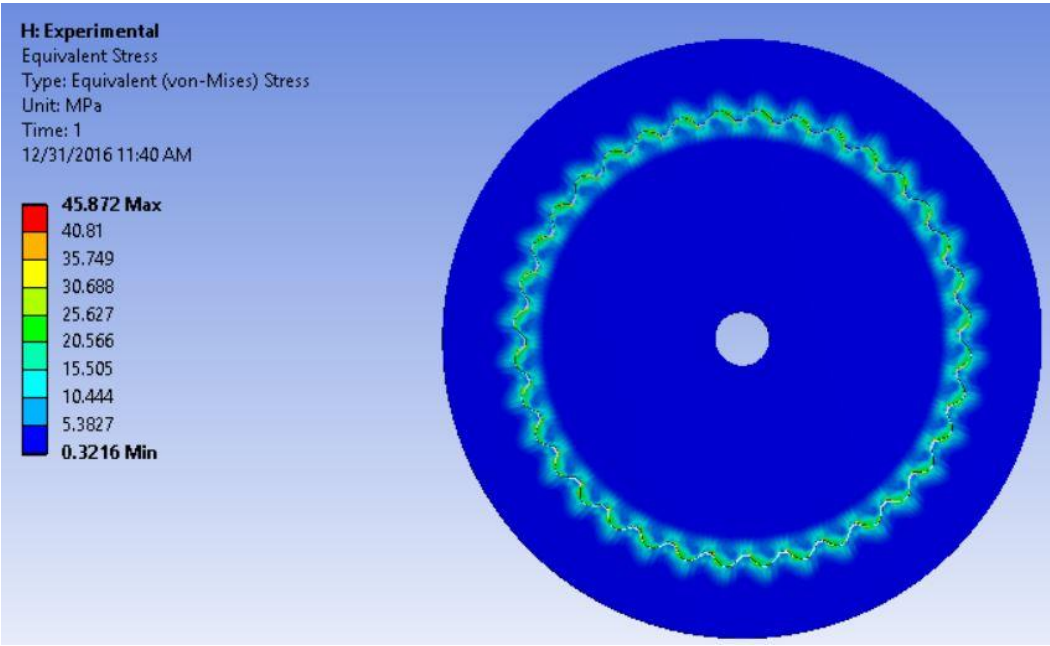


Figure 35: von-Mises Stress developed in the experimental model under load

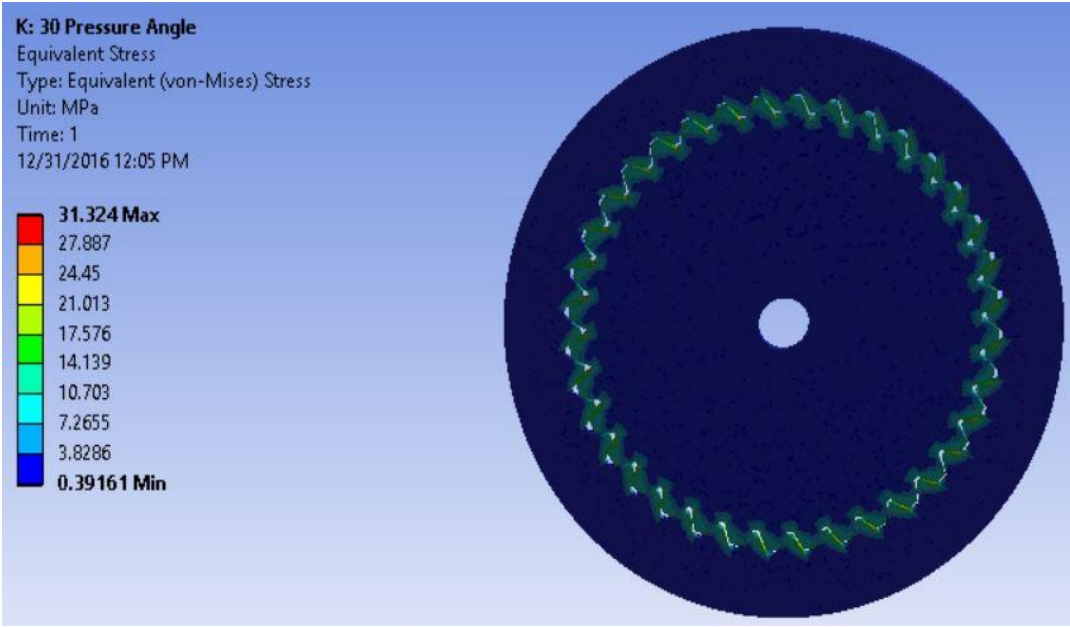


Figure 36: von-Mises Stress developed in the Improved model under load

6.7 Comparison of Equivalent Strain of the Experimental and Improved Model under load

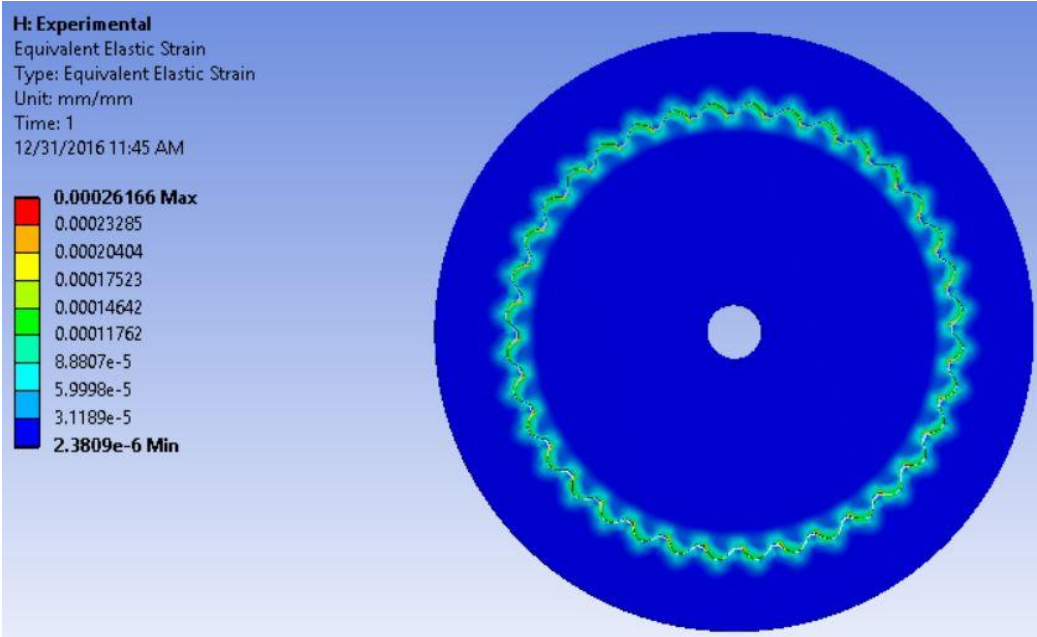


Figure 37: Equivalent Strain developed in the Experimental model under load

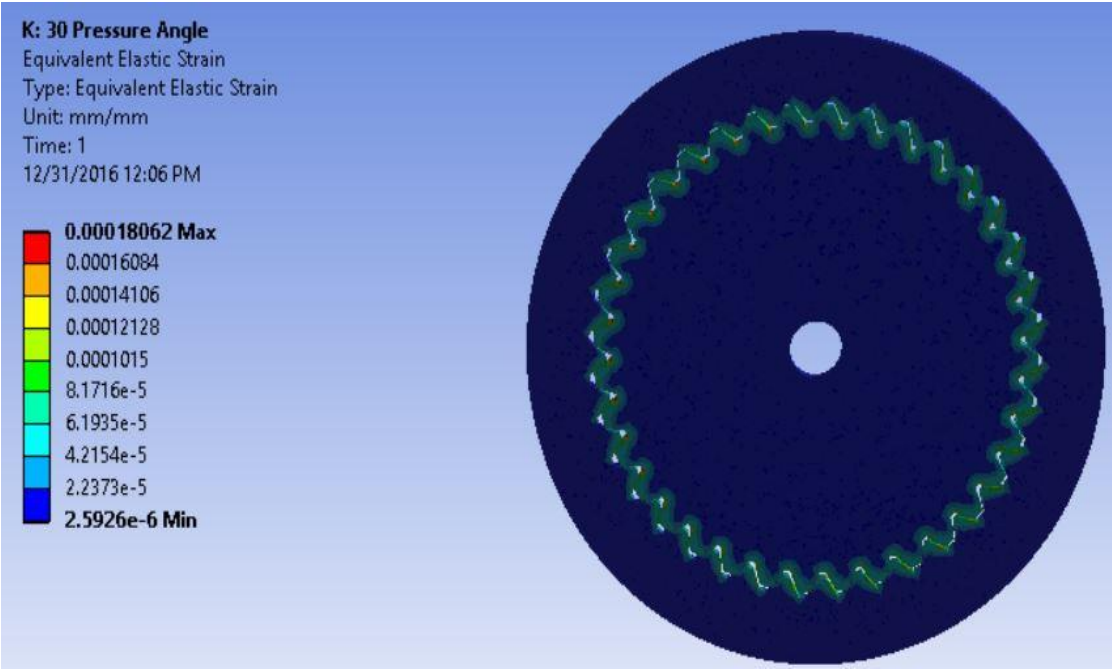


Figure 38: Equivalent Strain developed in the Improved model under load

6.8 Comparison of Total Deformation of the Experimental and Improved Model under load

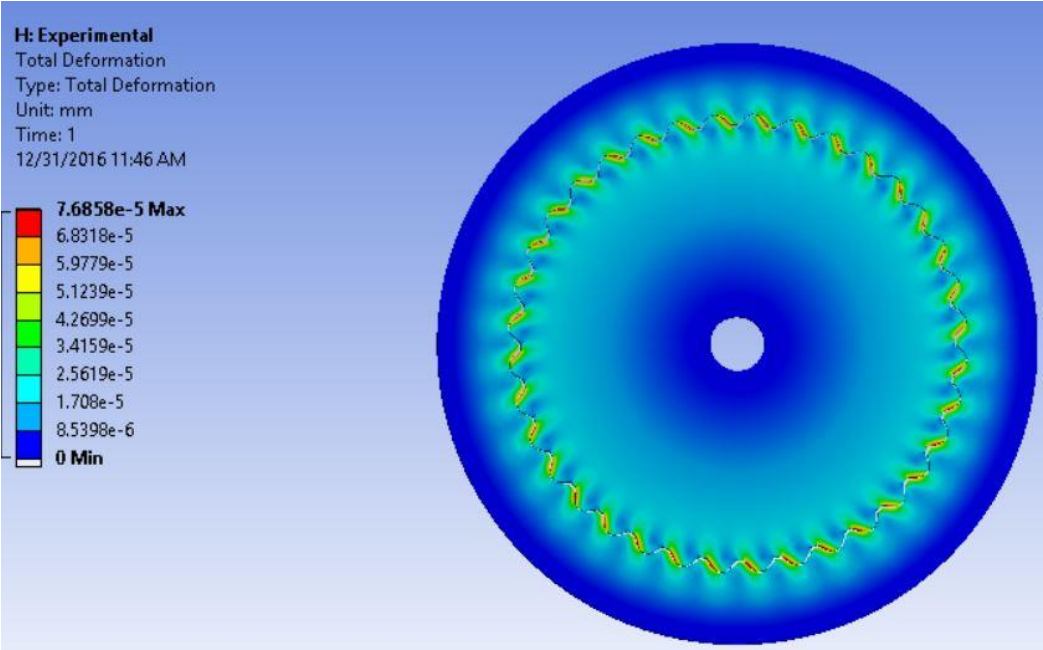


Figure 39: Total Deformation occurring in the Experimental model under load

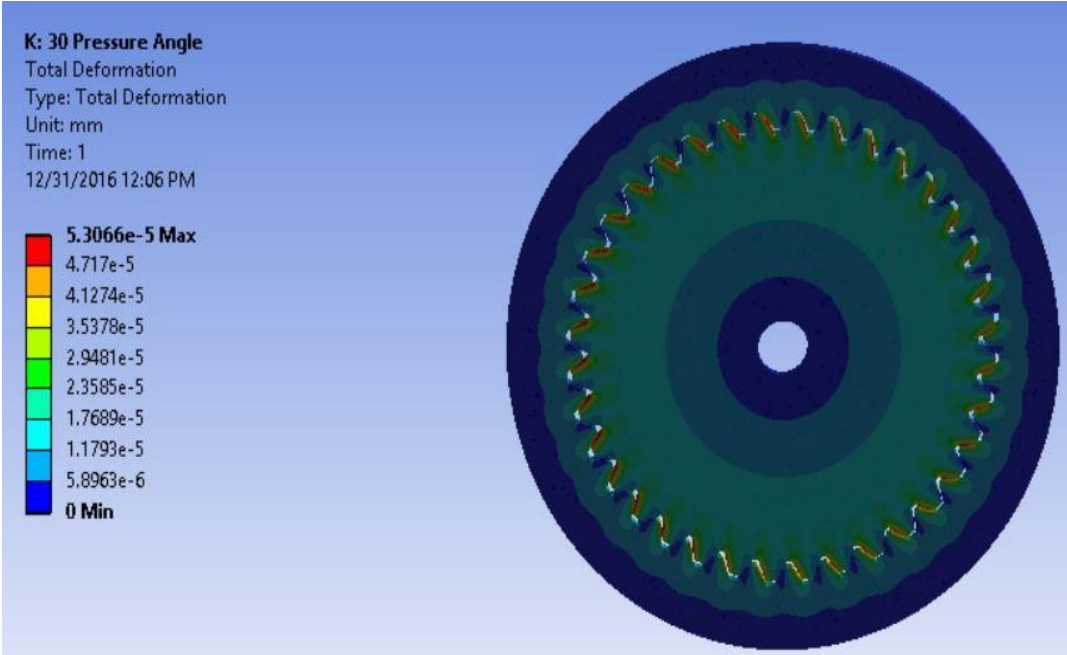


Figure 40: Total Deformation occurring in the Improved model under load

7.CONCLUSION

The investigation made on the real-time shaft which has considered in the study provides various information which is necessary to design the telescopic splined shaft with better performance. From the results obtained, the following conclusions are made.

- From the chemical analysis made, it was found that the material which is used in the real-time application is SAE 4140 steel grade.
- From the manual measurement, the outer diameter of the external spline shaft noted is 17.5 mm and the outer housing of the internal spline shaft is 22 mm.
- By analysing the experimental model of the shaft, the tolerance class found was Class 7 which also matches with the mathematically calculated tolerance value $(T+\lambda)$, 0.129 mm.
- From the static structural analysis results, it was found that the contact stress at the tooth sides is the major reason for wear and backlash.
- The analysis shows that the Stress-strain value of calculated model is double the value obtained in the experimental model which denotes the tolerance value has an impact on contact stress generation.
- By changing the module from 0.4535 to 0.3, the number of teeth is increased to 50 which improves the load distribution on the teeth. The contact stress developed is reduced to 40.34 MPa. As the top of the tooth, width is less, it provides sharp teeth which increase the risk of damage. So, it is not considered.
- The Min-Max value tolerance reduces the stress-strain on the teeth but the reduced tooth thickness will also lead to breakage. So, this improvement is not providing a better response.
- The formation of the serration teeth instead of involute teeth provides the good results compared to the theoretical model, but it is not recommended.
- From the various models produced, the contact stress developed by changing the pressure angle from 45° to 30° with theoretical tolerance is 31.32 MPa which is lesser than other models took into consideration. So, the improved telescopic spline shaft with 30° pressure angle is the best substitute for the experimental shaft which is taken in the study.

- The telescopic splined shaft with the pressure angle of 30° will provide the better performance in both hydraulic power steering and C-EPS system of steering compared to the present design procedures in use.

8.FUTURE SCOPE

Further studies are needed to conduct on improving the telescopic splined shaft by considering the surface treatment and improving the material properties such as hardness, wear and corrosion resistance. Improved shaft with good wear resistance is obtained on substituting Aluminium alloys instead of SAE 4140 because the coefficient of friction of the aluminium is less compared to the steel. But in case of accidents, the sudden increase of axial loading on the shaft will increase the risk of bending and leads to shaft failure. So, it is important to improve the splined shaft with better wear resistance, durability and strength to withstand axial loading condition. As backlash is the major problem, the introduction of splined brake pad arrangement supported by the compression spring between the internal and external splined shaft is the another innovative idea which is under consideration.

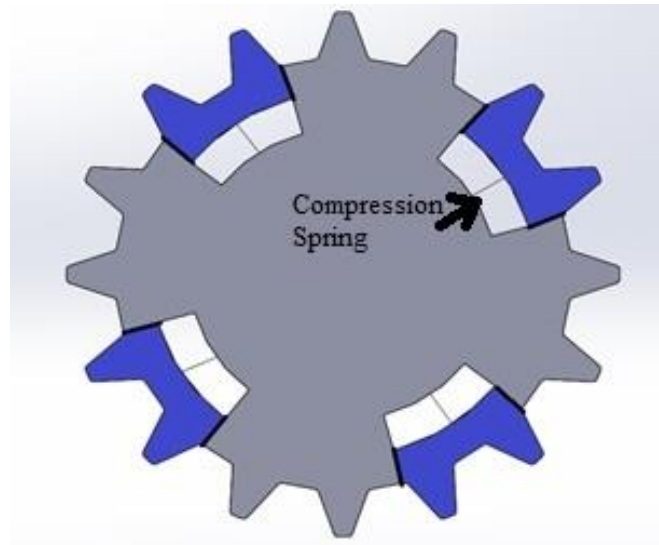


Figure 41: Proposed idea with the implementation of splined pad with compression spring

REFERENCE

1. Splines and Serrations - S.A.E. Standard Spline Fitting- ANSI B92.1-1970 (R 1993)
2. Jacek Krocak, Marian Dudziak., Tolerance Analysis of Involute splines, WCE 2011, July 6 - 8, 2011, London, U.K.
3. (United States of America Patent No. US20120080258 A1, Apr 5, 2012).
4. Guide to the use of tables and formulas in Machinery's Handbook, 27th Edition
5. Cook, Robert D., Warren C. Young. Advanced Mechanics of Materials. Macmillan, 1985.
6. Algor, Technical Documentation Access and Search (Docutech), v. 2.16 WIN, 1997 (CD-ROM).
7. Cedoz, R.W., M.R. Chaplin. Design Guide for Involute Splines, Society of Automotive Engineers, 1994
8. Buckingham, Earle (1935). Manual of Gear Design Section Two, The Industrial Press.
9. Colbourne, John R., (1987). The Geometry of Involute Gears, Quinn Woodine.
10. Michalec, George W., Precision Gearing: Theory and Practice, John Wiler & Sons, Inc, 1966.
11. (BUREAU OF INDIAN STANDARDS , March 1967)
12. American Standard ANSI B32.100 – 2005 Standard, Involute Splines, Metric Module.
13. I. Barsoum, F. Khan, Z. Barsoum. Analysis of the torsional strength of hardened splined shafts. (2013)
14. Khiralla, Tofa.W., (1976). On the Geometry of External Involute Spur Gears, C/I Learning.
15. Frictional coefficient of various material combinations [online cit.: 2016-09-02]. Available from http://www.engineeringtoolbox.com/friction-coefficients-d_778.html
16. Advantages of Involute Splines as Compared to Straight Sided Splines [online cit.: 2016-09-04] Article by Tiko Spline, Inc. Wixom, MI
17. Dimitri Kececioglu. Reliability Engineering Handbook, Volume 2, pp. 488-495, Pennsylvania, USA 2002.
18. Tooth breakage occurring in the splined shaft [online cit.: 2016-09-02]. Available from <http://www.motobrick.com/index.php?topic=490.0>
19. **H.Ueda.** Technical Trends regarding Intermediate shaft in steering systems, Koyo Engineering Journal, No. 168, pp. 14-17, 2005.

20. Scott Dearing. Heat treatment of steel Engineering Materials – ENGR 45, Nov 7, 2011
21. Francesca Curà, Andrea Mura. Analysis of a load application point in spline coupling teeth, Vol.15 No.4 P.302-308, Journal of Zhejiang University Science A 2014.

APPENDIXES



(a)

(b)

Figure 42: Internal Spline Shaft (a) and External Spline Shaft (b)

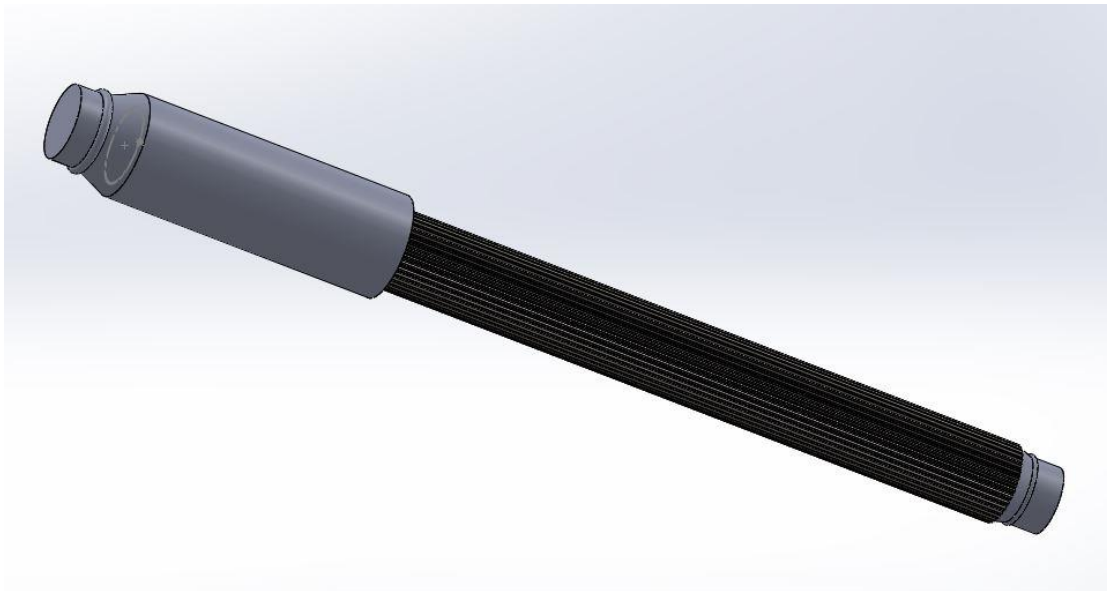
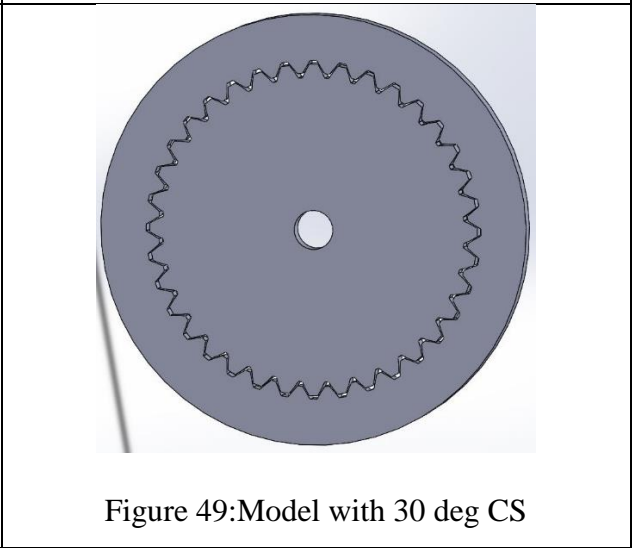
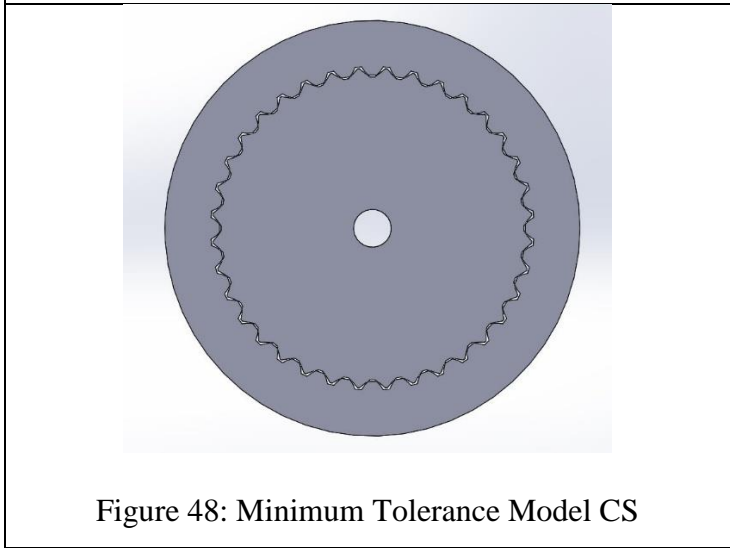
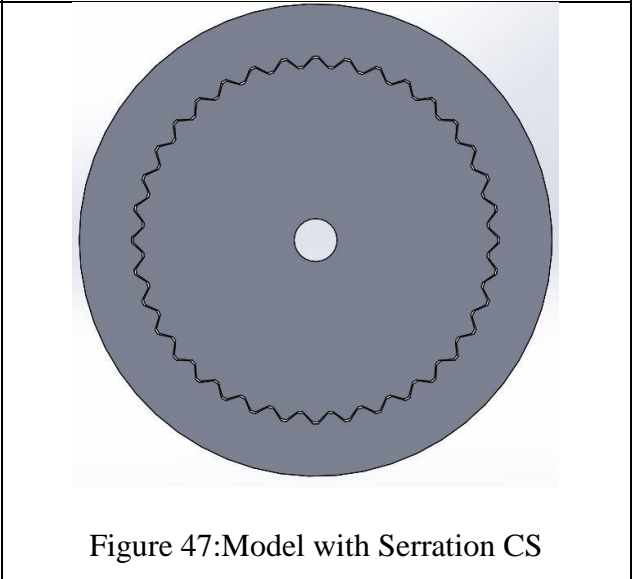
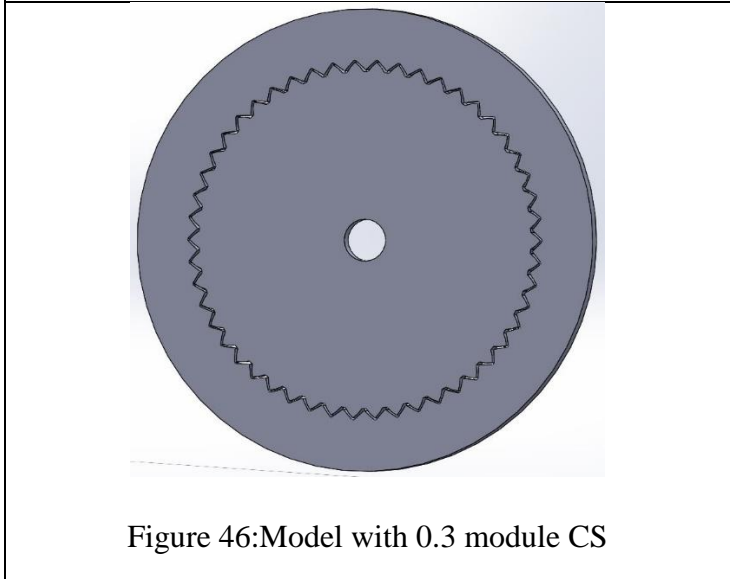
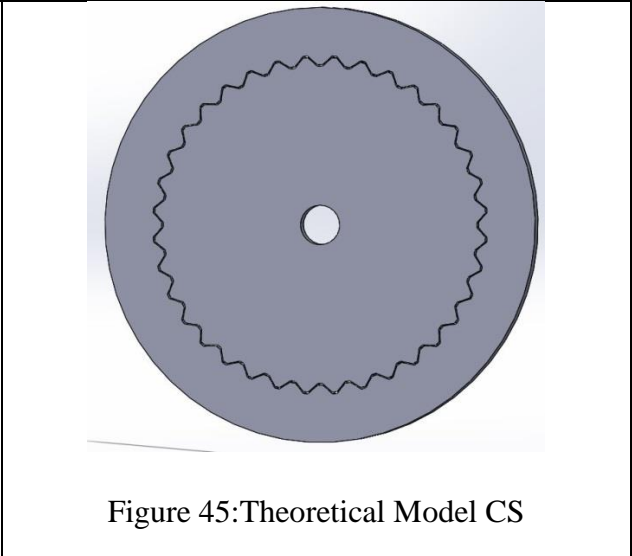
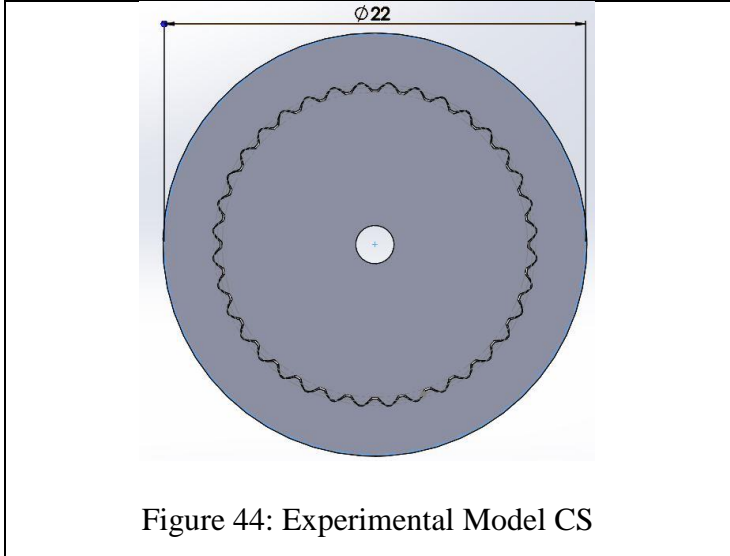


Figure 43: Experimental Telescopic Intermediate Splined Shaft



*CS refers to Cross Section